Paper II

*The influence of the edge beam on the
structural behavior of bridge deck overhangs*

Veganzones Muñoz, José Javier; Pacoste, Costin;
Pettersson, Lars; and Karoumi, Raid.

Manuscript to be submitted.

The influence of the edge beam on the structural behaviour of bridge overhangs

José Javier Veganzones Muñoz [a]*

Telephone 0046 8 790 86 57 / Email: jjvm@byv.kth.se

Costin Pacoste [a,c]

Telephone 0046 85 800 91 88 / Email: costin.pacoste@elu.se

Lars Pettersson [a,b]

Telephone 0046 10 448 11 56 / Email: lars.g.pettersson@skanska.se

Raid Karoumi [a]

Telephone 0046 8 790 90 84 / Email: raid.karoumi@byv.kth.se

[a] *Division of Structural Engineering and Bridges, KTH Royal Institute of Technology, Brinellvägen 23, SE-100 44, Stockholm, Sweden.*

[b] *Skanska Sweden AB, Major Projects, SE-112 74 Stockholm, Sweden.*

[c] *ELU Konsult AB, SE-115 31 Stockholm, Sweden.*

* Corresponding author. Email: jjvm@byv.kth.se

ABSTRACT

Bridge edge beams in Sweden may incur up to 60% of the life-cycle measures along the bridge's life span. In addition, road works results in traffic disturbances and, thus, increased user costs. Consequently, the Swedish Transport Administration started a project to develop solutions that can become better for the society in terms of cost. A life-cycle cost analysis was carried out to evaluate which proposals could qualify for more detailed studies and a demonstration project. The results showed that a solution without edge beam may result optimal. Even though such design solution might still fulfill the functional requirements of the edge beam, a structural analysis should be performed to evaluate its robustness.

The aim of this paper is to study the influence of the edge beam on the structural behavior of bridge deck slab overhangs. A non-linear 3D finite element model in the commercial software ABAQUS was developed for this purpose and validated using experimental data available in the literature. The load-displacement curves and the failure modes are observed. The shear and bending moment capacity of the overhang is studied. An assessment of existing design methods is presented in light of the load capacity obtained for each case.

The results show that the edge beam contributes to a higher load capacity of the bridge overhang than of that without edge beam. The shear capacity of the slab is more efficiently distributed, due to a stiffening effect in the critical cross section close to the transversal free edge. Therefore, the effect of removing the edge beam should be investigated for the bridge case at hand to account for the loss of robustness compared to a case with an edge beam. Existing design methods should be reviewed in order to account for the influence of an edge beam.

Keywords: bridge edge beam, bridge overhang, cantilever, structural analysis, finite-element model, shear force, bending moment, distribution width, failure mode.

Abbreviations: finite element (FE), reinforced concrete (RC), critical section (CS), edge beam (EB), without edge beam (nEB)

LIST OF SYMBOLS

Lower case Roman letters

a	Length of the bridge overhang
b_x	Width of the load application in x-direction
b_y	Width of the load application in y-direction
b_{eb}	Width of the edge beam
c	Distance of the load application point from the bridge overhang root
d	Effective depth at the considered cross-section
e	Eccentricity for the concrete damaged plasticity model
f	Coefficient for the Homberg-Rompers diagrams
f_c	Compressive strength of concrete measured on cylinders
f_{ct}	Tensile strength of concrete
f_u	Tensile strength of reinforcement
f_y	Yield strength of reinforcement
h_{eb}	Height of the edge beam
m_y	Bending moment per unit length in the y-direction
t_1	Height of the slab at the root of the overhang without edge beam
t_2	Height of the slab at the free edge of the overhang without edge beam
t_p	Thickness of the overlay (pavement)
x_u	Height of the compression zone
w_{eff}	Effective distribution width
w_m	Distribution width for bending moments
w_s	Distribution width for shear forces
w_p	Control perimeter for a punching shear force
y_{cs}	Distance from the center of the load application to the root of the overhang

Upper case Roman letters

$C_{Rd,c}$	Coefficient that depends on experimental tests (shear strength of concrete)
E_c	Elastic modulus of concrete
E_s	Elastic modulus of steel
M	Bending moment
M_x	Longitudinal bending moment of the edge beam in the x-direction
P	A arbitrarily placed concentrated load acting on the bridge overhang
Q_{Rd}	Load resisting capacity
V	Shear force
V_{td}	Bottom tensile reinforcement chord (shear resistance)
V_d	Design shear force per unit width

Lower case Greek letters

α	Direction of the principal resultant shear force
v_0	Principal resultant shear force per unit
v_d	Design shear force per unit width
v_{pav}	Shear force per unit width due to the surfacing.
v_{perm}	Shear force per unit width due to the other permanent loads.
v_Q	Shear force per unit length due to a (group of) concentrated load(s),
v_{SW}	Shear force per unit width due to the self-weight
v_x	Shear force per unit width acting in the x-direction
v_y	Shear force per unit length acting in the y-direction
v_{Rd}	Nominal shear resisting capacity of concrete per unit width
ξ	Factor accounting for the size effect in shear strength
ρ_l	Flexural reinforcement ratio

1. INTRODUCTION

Bridge edge beams have recently been a matter of study in Sweden. The Swedish Transport Administration (in Swedish, "Trafikverket") started a project to develop new bridge edge beam solutions that could become better for the society in terms of costs. The rationale was the heavy deterioration observed which resulted in high life-cycle measure costs in terms of repairs and replacements. At the same time, road disturbances are caused, i.e., user costs. In total, 25 proposals were presented and grouped into four types:

- Type I: Concrete integrated edge beam
- Type II: Without edge beam
- Type III: Steel edge beam
- Type IV: Concrete prefabricated edge beam

These proposals are described in detail in Pettersson & Sundquist (2014). Type I is the Swedish standard design. A type IV proposal where the edge beam is cast *in situ* and then lifted to the bridge formwork where the deck is subsequently cast has successfully been constructed recently in Sweden (Kelindeman, 2014). A life-cycle cost analysis (LCCA) was performed to evaluate and compare the different edge bean types (Veganzones, Sundquist, Pettersson, & Karoumi, 2015). A representative design solution for each type was chosen. The study concluded that type I may be an adequate solution for long bridges, whereas type IV is for short bridges.

Nevertheless, there is still room for improvement. In addition to the damage remarks documented along the life span, the working conditions referred to Type I in the construction of the new bridge or the replacement of an existing deteriorated edge beam are not favorable (**Figure 1**). This fact may lead to worse quality in the edge beam and, therefore, shorter life span. Type IV contributes to enhanced working conditions which results in extended life span, but the replacement is not optimal.

Figure 1: a) Construction and b) replacement of a Type I edge beam

The LCCA showed that uncertainties existed for Types II and III. Such solutions could become better from a LCCA perspective under certain scenarios. Type III results in higher investment costs, but low life-cycle measures costs, mainly because it enables a faster edge beam replacement. This fact has motivated Trafikverket to consider this type for further detailed studies and implement it as means of replacement of a damaged edge beam in a bridge in Sweden. The works are planned for execution in spring 2016 (Ramos, 2015).

In order to provide enhanced working conditions during the bridge construction the option of not having an actual edge beam (Type II) turns out to be interesting. **Figure 2** shows three design solution proposals without edge beam from the edge beam group. In absence of an actual edge beam, these

proposals still need to fulfill basic requirements such as provide an adequate attachment for the railing, support the bridge deck overlay and contribute to the drainage system.

In Type IIa, an L-shaped profile is placed to support the overlay and to lead the water to the drainage system. The railing is attached from the side of the bridge deck slab. An alternative where the railing attachment is from the top – as it is nowadays in Sweden – is represented by Type IIb. It has a similar design as Type IIa, but with steel supports at each railing post location instead. Type IIc, which can also be considered as Type III – steel edge beam –, consists of a continuous L-shaped profile where the railing is attached and fulfills the rest of the requirements aforementioned. The LCCA was carried out for Type IIb and showed that the investment costs resulted low. In contrast, the life-cycle measure costs became very high due to the maintenance of 1) the steel support, because of the contact surface with the concrete deck slab and, 2) the L-steel profile because of the damaged caused by the snow removal machine.
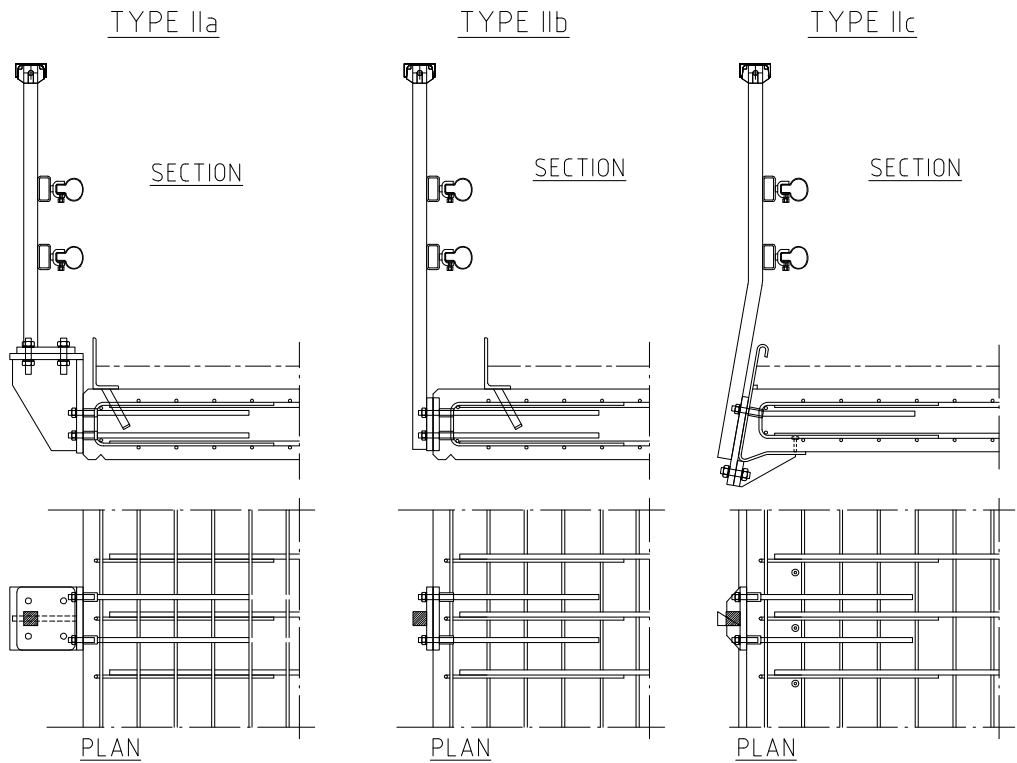

Figure 2: Design solution proposals without edge beam

Nevertheless, the effects from removing the edge beam should be studied in detail, especially for bridges with overhangs (**Figure 3**). The reason is that the edge beam also serves to distribute concentrated loads from the traffic. Smith & Mikelsteins (1988) showed that the presence of an edge beam affects the load distribution and indicated that a refined method of analysis including such effect should exist. Vaz Rodrigues R. (2007) investigated the influence of different edge beam sizes (including without edge beam) from a structural point of view on reinforced concrete (RC) slabs, and confirmed that the stiffening effect of the edge beam is related with its load-carrying function. A considerable reduction of the total shear force near to the free edge was observed through a linear-elastic finite element (FE) model. Nevertheless, the positive influence of an edge beam is not currently accounted for in the existing regulations in Sweden.
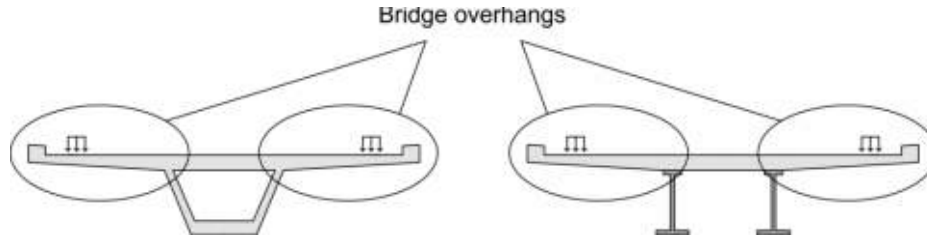
Figure 3: Overhangs in a cross-sectional box beam bridge and a slab-on-girder idealized structurally as cantilever slabs

The aim of this paper is to study the possibility of implementation of a solution without edge beam that fulfills functional requirements and is robust from a structural point of view. The goal is to analyze the influence of the edge beam on the structural behavior of the bridge overhang's concrete slab. The objective is the assessment of the total load resisting capacity for a case of a bridge overhang under concentrated loads considering the presence and absence of an edge beam. A non-linear 3D FE-model that can describe the failure of the bridge overhang has been developed and validated for this purpose. The efficiency and adequacy of different design methods used to calculate the design bending moment and the shear force developed in the critical areas of the overhang in the ultimate limit state is analyzed. A review of the development of simplified calculation methods is presented. Experimental tests concerning RC cantilever slabs under concentrated loads available in the literature are described. The load capacity obtained from experimental tests, linear-elastic and non-linear FE-models and simplified design methods are compared and discussed. A reflection on the old Swedish Code BB94 and the use of distribution widths according to the design recommendations is presented. Possible consequences of the removal of the edge beam are mentioned.

2. REVIEW OF CALCULATION METHODS FOR RC BRIDGE OVERHANG SLABS

Overhangs in bridges as shown in **Figure 3** have traditionally been structurally idealized as cantilever slabs (Bakht, 1981). Nevertheless, the assumption of full rotational restraint at the root may lead to an overestimation of the peak intensity of the transversal moment (Mufti, Bakht, & Jaeger, 1993). Bridge overhangs are usually designed with a tapered thickness (haunch) across the slab decreasing from the root towards the free edge, ending in an edge beam (**Figure 4**).
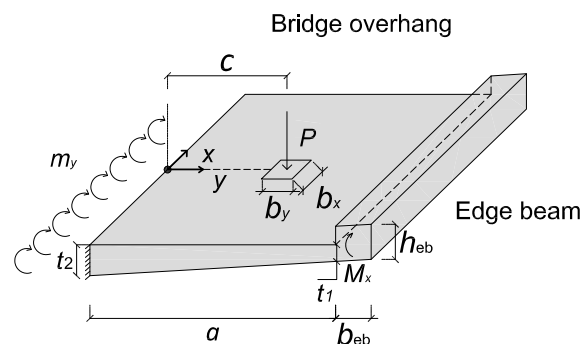

Figure 4: Bridge overhang idealized as a cantilever slab subjected to a concentrated load from a vehicle P applied at a distance c from the overhang root of a length a

Either by using a classical simplified method or a linear-elastic FE-analysis, the design values for the transversal bending moment per unit width along x-axis ($m_{y,d}$), longitudinal bending moment of the edge beam ($M_{x,d}$) and the principal shear force per unit width ($v_{0,d}$) in the critical cross sections considered can be calculated. Unrealistic concentrations of cross-sectional moments and shear forces occur due to the fact that necessary simplifications may occur in FE-modelling (Pacoste, Plos, & Johansson, 2012). Furthermore, the redistribution of forces prior to failure should be considered.

3

Thus, the maximum value calculated should not be used as the design value. The use of distribution widths instead are contemplated in this study. A brief review of simplified calculation methods for RC cantilever slabs and recommended values of distribution widths is presented for bending moment and shear force. The notations illustrated in **Figure 4** are used.

2.1 BENDING MOMENT

2.1.1 Simplified lower-bound calculation methods

Beam theory based

Wästlund (1964) proposed a simplified model to evaluate $m_y(x)$ and $M_x(x)$ for a concentrated load P applied on the edge beam. The cantilever slab was divided into plate strips. These were considered as an elastic foundation supporting the edge beam. A parameter that depends on the moment of inertia per unit length of the plate strip, the moment of inertia of the edge beam and a factor accounting for a tapered thickness was introduced. Maximum values for m_y, and maximum and minimum values for M_x were presented.

Plate theory based

Jaramillo (1950) presented the exact solution in terms of proper integrals for $m_y(x)$ using plate theory in an infinitely long cantilever plate of constant width and thickness due to a concentrated load acting at an arbitrary point. The edge beam was not considered. The solution was transformed into series form by means of contour integration. Pucher (1951) presented influence surfaces for the calculation of $m_{y,\max}$ at the root of the bridge cantilever for constant thickness slabs. Classical plate theory assuming small deflections and no shear deformations was used. Homberg & Ropers (1965) extended this work by including variable linear and parabolic thicknesses and multiple spans, including cantilevers (**Figure 5**). The edge beam can be accounted for by extending the concrete slab with a portion equivalent to its flexural rigidity. This approach should be handled with care since it might lead to inaccurate results. The value of $m_{y,\max}$ is derived by placing the concentrated load P on the influence surface using the conforming scale. The corresponding contour level of the influence surface will indicate the coefficient f used for the calculation of $m_{y,\max}$ (**Eq. 1**). In case of multiple n loads several f_n can be used (**Eq. 2**).

$$m_{y,\max} = f\,P \qquad\qquad (\text{Eq. 1})$$

$$m_{y,\max} = \sum_{i=0}^{n} f_n\,P_n \qquad\qquad (\text{Eq. 2})$$

Reismann & Cheng (1970) extended the problem postulated by Jaramillo including an edge beam bonded to the free edge of the cantilever plate. The concentrated load P was applied on the edge beam. Plate/edge beam stiffness ratios in bending and torsion were used. The results were expressed in terms of improper integrals and evaluated by a numerical integration procedure. In order to prevent using improper integrals, Sundquist (2010) presented a simplified solution assuming the transverse free edges of the cantilever to be simply supported. A generic solution in terms of Fourier series was obtained for $m_{y,\max}$ and $M_{x,\max}$. Sundquist (2010) showed that Wästlund's solution using beam theory was more conservative compared to his solution based on plate-theory. A drawback of such methods is that the load shall be placed on the edge beam and not in an arbitrary point which has made it not very usable in practice.
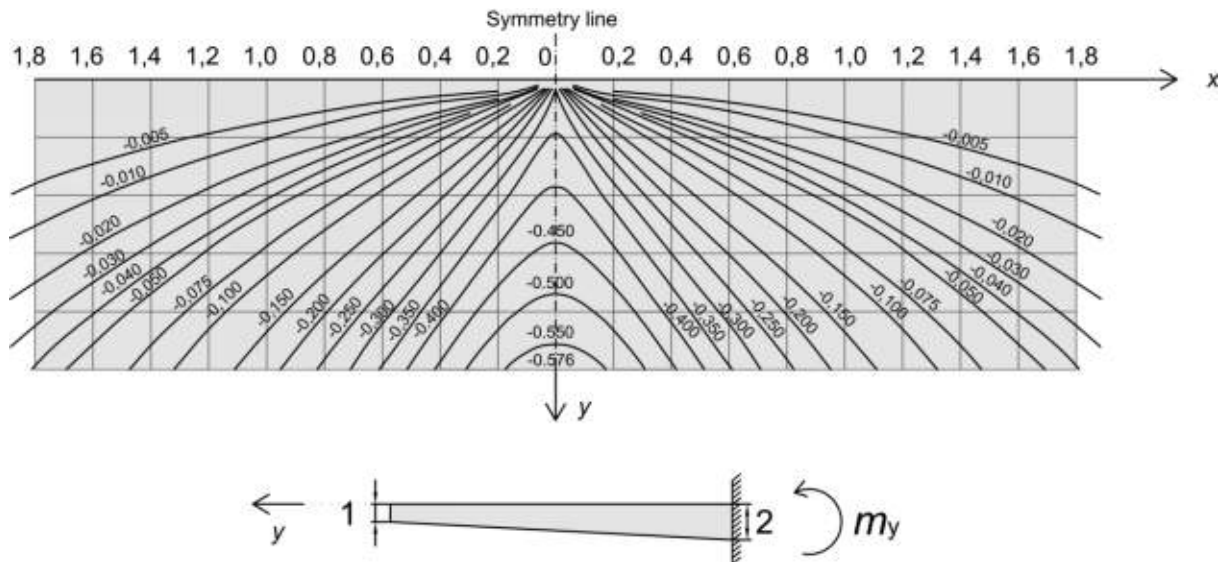
Figure 5: Example of an influence surface for the calculation of the transversal bending moment at the cantilever root for a thickness variation of $t_2/t_1 = 2$ Reproduced from Homberg & Ropers (1965).

FE-model based

Bakht & Holland (1976) presented a semi-graphical simplified solution for the elastic analysis of infinite wide cantilever slabs of linearly varying thickness. The distribution of $m_y(x, y)$ at any point of the cantilever slab can be calculated. A coefficient that depends on the relative position of the load, the reference point with respect to the root of the cantilever and, if applicable, the slab/edge beam stiffness ratios was presented in design charts. This coefficient was back-calculated from linear-elastic FE-models. Later, Bakht (1981) also introduced a similar method to calculate $M_{x,\max}$ and $M_{x,\min}$. The current Canadian code (Canadian Standards Association, 2015) uses this formulation.

The assumption of a full fixity versus the consideration of the presence of the web and the portion of the deck in between the webs was investigated by Dilger, Tadros, & Chebib (1990). It was observed that moments could become higher by up to 40% for thin webs. Similar design charts completed later by Mufti, Bakht, & Jaeger (1993) were presented including a parameter to represent the elastic restraint for the cantilever slab.

2.1.2 Linear-elastic FE-analysis

Moments achieved through linear elastic FE-analysis may be redistributed because of the plastic rotation capacity of concrete according to Eurocode 2 (European Committee for Standardization [CEN], 2005). The resulting distribution must remain in equilibrium with the applied loads. However, currently there is no clear formulation for the distribution width (w_m) for m_y. Designers instead usually account for $m_{y,\max}$ as the design value ($m_{y,d}$). Pacoste et. al (2012) proposed recommendations for the calculation of w_m for FE-analysis (**Eq. 3**) in the critical cross section as depicted in **Figure 6a**. For loading situations involving two parallel forces so that the distribution widths overlaps, a distribution width (w_{mR}) can be used according to **Eq. 4** and **Figure 6b.** Even though such recommendations were considered still conservative (Lim, 2013), the effect of plastic redistribution should be handled with care if there are moving loads that might cause accumulated damage to the structure, which might lead to additional plastic rotation.

$$w_\mathrm{m} = \begin{cases} \min\begin{cases} 7d + b_x + t_\mathrm{p} \\ 10d + 1{,}3y_\mathrm{cs} \end{cases} & \text{for} \begin{cases} 0{,}25 \geq \dfrac{x_\mathrm{u}}{d} \geq 0{,}15 \text{ for concrete classes} < \mathrm{C}55/67 \\ 0{,}15 \geq \dfrac{x_\mathrm{u}}{d} \geq 0{,}10 \text{ for concrete classes} \geq \mathrm{C}55/67 \end{cases} \\ \qquad 2h + b + t_\mathrm{p} \quad \text{for values of } \dfrac{x_\mathrm{u}}{d} \text{ outside the above limits} \end{cases} \qquad \text{(Eq. 3)}$$

$$w_\mathrm{R} = 2x_\mathrm{R} + w_\mathrm{m} \qquad \text{(Eq. 4)}$$

Where

- d is the effective height of the cross section studied.
- b_x is the width of the load in the x-direction.
- t_p is the thickness of the overlay.
- y_cs is the distance from the center of the load application to the critical cross section.
- x_u is the depth of the neutral axis in the ultimate limit state after redistribution evaluated for the section with the highest reinforcement ratio.
- x_R is the distance of the resultant force of both loads to the closest external force.
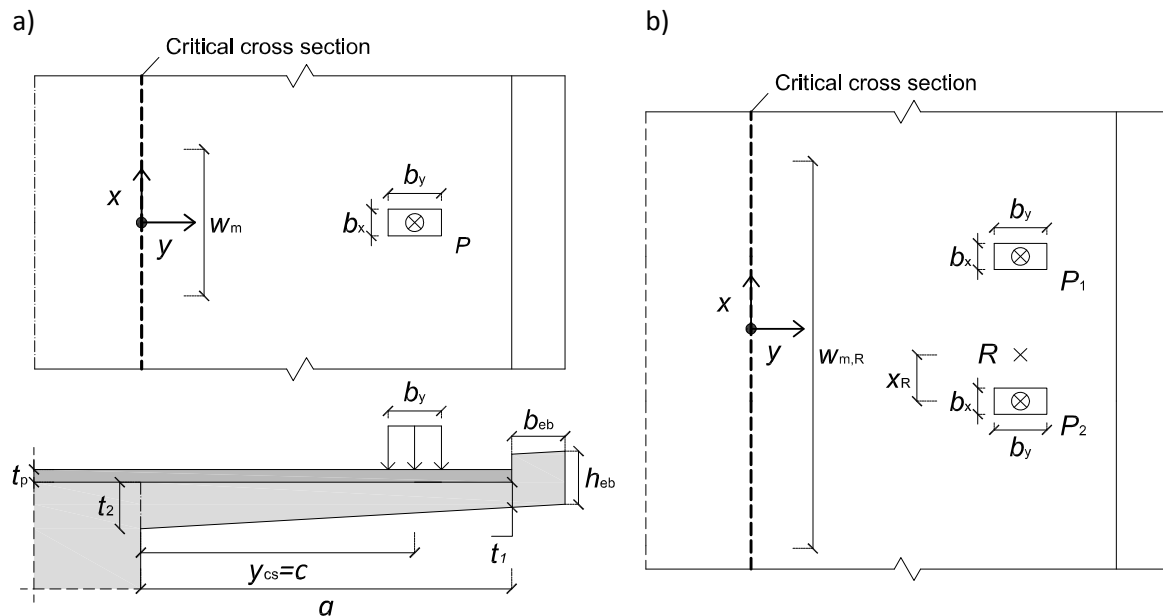

Figure 6: Shear distribution widths for a) one concentrated load and b) two concentrated loads

2.2 SHEAR FORCE

2.2.1 Shear strength of RC slabs

Shear is usually the governing failure mode in the ultimate limit state of RC slabs without transverse reinforcement (Muttoni, 2008). Two types of shear failure modes are usually distinguished: one-way shear and two-way shear (punching). The former is associated with line loads and linear supports. The latter is usually related to concentrated loads. In both cases the failure is brittle and undesirable. For RC bridge overhangs, Vaz Rodrigues R. (2007) stated that a hybrid failure between both occurs and indicated that the design for such intermediate case is not always covered by current codes of practice. A few experimental tests on RC cantilevers are described herein.

Miller, Aktan, & Shahrooz (1994) performed a test on a decommissioned concrete slab bridge under two concentrated loads. The bridge failed in shear. Yield was observed just before failure. Ibell &

Morley (1999) carried out series of full scale tests on a concrete beam-and-slab bridge deck with no shear reinforcement under concentrated loads. The specimens failed in shear and no or limited yielding was documented. Lu (2003) carried out a series of nine tests on reduced scale RC cantilever without stirrups. Different reinforcement ratios and load configurations and the effect of an edge beam were studied. The predominant failure was shear. For the case of the edge beam an increase of the load capacity and slightly more ductile behavior was documented. The shear crack did not go through the edge beam but developed in the area within the slab instead.

Vaz Rodrigues R. (2007) investigated the shear strength of RC bridge deck slabs without shear reinforcement. Six large-scale tests on two cantilevers with different load configurations and flexural reinforcement ratios were carried out. A brittle shear failure was observed. The theoretical flexural failure load was not reached. The failure load increased with the number of applied loads. For the tests performed with the same number of loads, the failure load decreased with the reinforcement ratio. Significant yielding occurred in top and bottom reinforcement for the test configuation with four concentrated loads. For the rest of the tests no or very limited yielding was reported. The critical shear cracks did not seem to form from the existing flexural cracks.

Rombach & Latte (2008) conducted 12 large-scale tests on four specimens. The influences of stirrups and a tapered thickness were studied. This latter refers to the consideration of a concrete compression chord (V_{ccd}) and/or a reinforcement tensile chord (V_{td}) to contribute to the shear resistance (**Figure 7**). A spontaneous brittle shear failure was observed for the cantilever slabs without stirrups. The bending reinforcement did not yield. The load capacity measured was higher than the design one. The specimens with stirrups had a ductile bending failure, with a considerable yielding plateau. The influence of the tapered thickness was almost not perceptible, which led to the performance of new tests in single supported beams (Rombach, Kohl, & Nghiep, 2011). The contribution of the concrete compressed chord was studied as means of inclining the top part with varying angles (0-10°). A brittle spontaneous shear failure was documented among great part of the slabs, except the ones with higher angle of inclination which had a bending failure. In terms of load capacity, the consideration of such positive influence could lead to unsafe results for designing concrete members with varying depth without shear reinforcement.
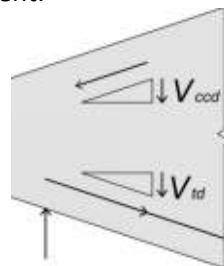

Figure 7: Shear components for members with inclined chords

The formulation corresponding to the Eurocode to calculate the shear capacity of RC slabs for different codes for the verification of the shear failure criterion is presented in **Appendix 1**. Members without shear reinforcement and without pre-stressing are referred. In this paper the old Swedish code BBK94 (Boverket, 1994) is studied to evaluate the load capacity of bridges designed following its guidance. In spite of experimental evidence, as far as it has been investigated, no formulae including the consideration of the edge beam for an increased shear strength capacity of concrete have been found in the literature. A recently discussed aspect is the consideration of the inclined chords (Zanuy & Gallego, 2015). Eurocode indicates that it should be considered for members with shear reinforcement. In some countries it is allowed for RC slabs without stirrups (Rombach & Kohl, 2013). Zanuy & Gallego (2015) concluded that it is not consistent to account for such effect when using the Eurocode because of the different background of both equations. In contrast, BBK94 highlighted that the positive or negative influence of a tapered height beam or slab should be accounted for.

2.2.3 Simplified calculation of the design shear force

Designers may adopt one of one-way or two-way shear criteria to calculate the load capacity (Q_{Rd}). Intuitively, the punching shear criterion should be used for a two-directional flow of shear forces, which can be the case of loads applied to the free edge. In contrast, a one-way shear criterion should be adopted for a unidirectional flow, which can be the case of loads applied close to the root of the overhang. Vaz Rodrigues R. (2007) concluded that both approaches for different load positions may result suitable because of the hybrid nature of the failure.

One-way shear criterion

The authors believe that the consideration of one-way shear criterion in a local analysis can be considered adequate even for forces applied close to the transversal free edge if only the predominant direction of the principal shear perpendicular to the root of the overhang is considered. A global analysis should account for shear along the other direction. The design shear force per unit length v_d for one-way shear can be derived according to **Eq. 5**. The shear force per unit length (v_Q) can be calculated along the critical cross section using the distribution width (w_s) following **Eq. 6** as illustrated in **Figure 8b**.

$$v_d = v_Q + v_{SW} + v_{pav} + v_{perm} < v_{Rd} \ [kN/m]$$

(Eq. 5)

$$v_Q = \frac{Q_d}{w_s} \ [kN/m]$$

(Eq. 6)

Where:
- v_Q is the shear force per unit length due to a (group of) concentrated load(s).
- v_{SW} is the shear force per unit length due to the self-weight.
- v_{pav} is the shear force per unit length due to the surfacing.
- v_{perm} is the shear force per unit length due to the other permanent loads.
- w_s is the distribution width for shear forces.

Distribution widths

The Swedish code Bro 11 (Trafikverket, 2011b) recommends calculating w_s according to **Eq. 7.** This formulation is originally based on the experimental tests made by Hedman & Losberg (1976). For loading situations involving two parallel forces where w_s overlap, an extended $w_{s,R}$ can be used as in **Figure 6b**. The critical cross sections depicted in **Figure 8b** are located at $d/2$ from the load pad (Trafikverket, 2011b).

$$w_{s,B11} = \max \begin{cases} 7d + b_x + t_p \\ 10d + 1{,}3y_{cs} \end{cases}$$

(Eq. 7)

Two-way shear design criterion

The shear design criterion is presented in **Eq. 8** where v_d is the design shear force per unit control perimeter (w_p). Because of the presence of a free edge, a three-sided critical control perimeter can be used in this problem (Vaz Rodrigues, Fernández Ruiz, & Muttoni, 2008). The critical cross section can be located at a distance $2d$ according to Eurocode (CEN, 2005), or $d/2$ according to ACI (ACI [American Concrete Institute], 2014), respectively (**Figure 9**).

$$v_\text{d} = v_\text{Q} + v_\text{SW} + v_\text{pav} + v_\text{perm} \; < v_\text{Rd} \; [\text{kN/m}]$$

(Eq. 8)

$$v_\text{Q} = \frac{Q_\text{d}}{w_\text{p}} \; [\text{kN/m}]$$

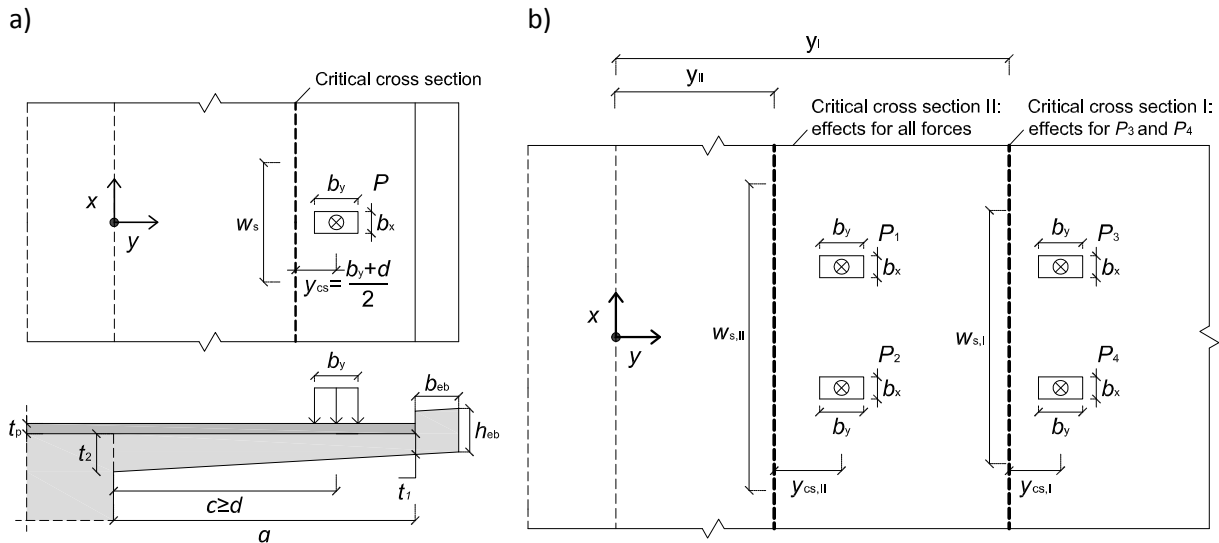a)   b)

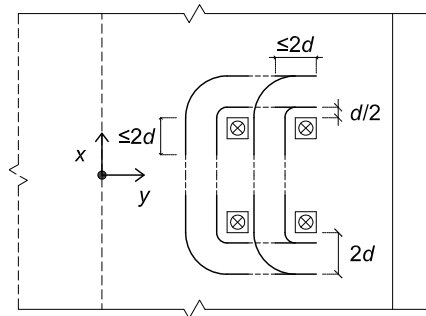**Figure 8. Distribution widths and critical cross sections for shear forces for a group of four concentrated loads**

Figure 9: Three-sided punching control perimeters at distances $2d$ or $d/2$ from the load application for a group of four concentrated loads

2.2.4 Linear-elastic FE-analysis

The redistribution of shear forces in linear-elastic FE-analyses refers to the resultant principal shear force v_0 (**Eq. 9**) and is performed in the x-direction. The principal shear force is assumed to verify the shear failure. Pacoste et. al. (2012) proposed refined recommendations for the shear distribution width, denoted as $w_\text{s,PPJ}$ (**Eq. 10**). All the existing load cases, including self-weight, are applied. Such recommendations have recently been shown to be reasonable (Shams Hakimi, 2012). A maximum and a minimum distribution width ($w_\text{s,max}$, $w_\text{s,min}$) are calculated for the hypothetical critical cross sections located closest to ($y = 0$) and furthest from ($y = y_\text{max}$) the root of the overhang. y_max accounts for a limiting distance (a_min) for the application of the load from the railing (**Figure 10a**). The distribution width ($w_\text{s,PPJ}$) for a load applied at a distance y from the root edge is calculated through linear interpolation between $w_\text{s,max}$ and $w_\text{s,min}$. A similar principle as **Figure 6b** is applied for two parallel forces to calculate a resultant distribution width $w_\text{R,s}$ (**Eq. 11**). A limiting condition for a calculation of an effective distribution width (w_eff) based on the angle (α) of the principal resultant shear forces is applied according to **Figure 11.** The rationale is to account for the shear forces distributed mainly in the y-direction.

$$v_0 = \sqrt{v_x{}^2 + v_y{}^2} \tag{Eq. 9}$$

$$w_{s,max} = max \begin{cases} 7d + b_x + t_p \\ 10d + 1{,}3y_{cs} \end{cases} \text{for } y = 0 \tag{Eq. 10}$$

$$w_{s,min} = min \begin{cases} 7d + b_x + t_p \\ 10d + 1{,}3y_{cs} \end{cases} \text{for } y = y_{max}$$

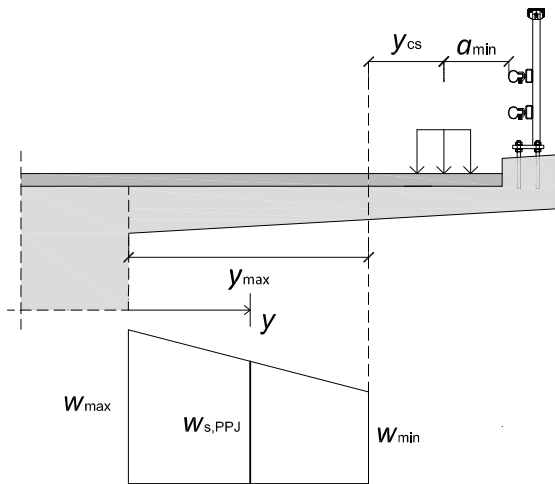$$w_{R,s,PPJ} = 2x_R + w_{x,s} \tag{Eq. 11}$$

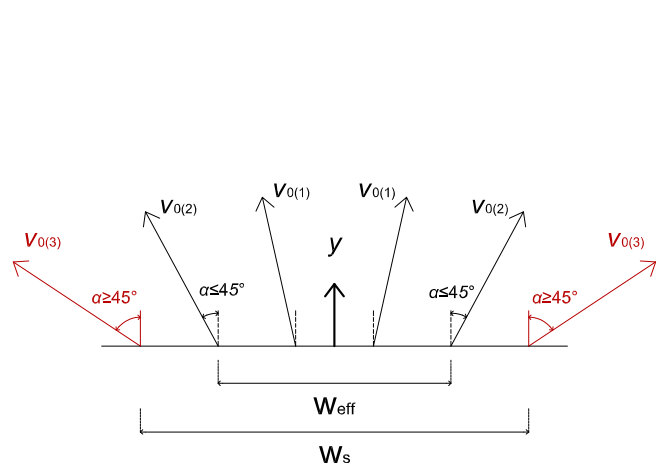**Figure 10: Interpolation of the calculation of the shear distribution width**

Figure 11: Limiting condition for the shear distribution width. Adapted from Pacoste et. al. (2012)

3. METHODOLOGY

In order to study the structural behavior of bridge overhangs with and without an edge beam the experimental tests carried out by Vaz Rodrigues R. (2007) were used as a reference. The reason for this choice is that, even though the tests correspond to a scale of ¾ of Swiss bridges in Switzerland, such dimensions resemble approximately the ones used in Sweden. The experiment consisted of three tests (DR1a, DR1b and DR1c) on the same RC slab performed successively. In test DR1a four concentrated loads were applied in the middle of the RC slab. In tests DR1b and DR1c, two and one concentrated loads respectively were applied in the area near the transverse free edge (**Figure 12**). An edge beam with the Swedish standard dimensions was included successively.

The load capacity (Q_{Rd}) for bending and shear according to the simplified methods aforementioned was calculated. Afterwards, Q_{Rd} from a 3D linear elastic FE-analysis was derived. These results were discussed in the light of the conclusions stated by Vaz Rodrigues R. (2007). The influence of the edge beam was studied as means of the distribution of shear forces and bending moments. The consideration of the redistribution through distribution widths is also discussed.

Subsequently, a 3D non-linear FE-model with solid elements was built to investigate the structural behavior of the bridge overhang in the ultimate limit state. The results were compared to the experimental tests to validate the FE-model as means of load-displacement curves and failure modes observed. The edge beam was added to investigate its influence on Q_{Rd}. A comparison and assessment

of the efficiency of the design methods presented to obtain Q_{Rd} compared to Q_{Rd} from non-linear FE-model and experimental tests was discussed.

ABAQUS/CAE, ABAQUS/Standard ad ABAQUS/Explicit Version 6.1.14 are the commercial software used for the FE-analyses. ABAQUS/CAE is used for the construction of the FE-model and the generation of the input file. ABAQUS/Standard is used to perform the elastic-linear analyses and ABAQUS/Explicit is used to perform the non-linear analysis, both generating the output files.

3.1 DESCRIPTION OF THE FE-model

General assumptions and limitations

- Bond slip between concrete and reinforcement was not considered. Since no anchorage failure was reported in the experiments this issue was not verified.
- The fluctuation of the load magnitude applied onto each plate during the experiment was not accounted for. The actual applied force under each load application point was actually measured in the test. In the FE-model the same load on each loading plate on the overhang was assumed.
- The initial load cycling in test DR1a has not been considered. A load-displacement curve for the comparison with the FE-model which does exclude this effect presented by Vaz Rodrigues R. , (2007) was used. Concerning tests DR1b and DR1c the successive steps of constant and increasing loading were not considered.

Geometry and reinforcement

The geometry of the model follows the experimental test by Vaz Rodrigues R. (2007) represented in **Figure 12.** The longitudinal reinforcement consists of two layers (top and bottom) of ⌀16 mm bars every 150 mm. The length of the cantilever is 10 m and the width is 4,2 m. The overhang has a tapered thickness at the root of the overhang t_2 of 380 mm and at the free edge t_1 of 190 mm. The transversal reinforcement is composed of ⌀12 mm every 150 mm, but shortened to 75 mm across a distance of 2800 mm from the left part of the slab (1400 mm from the overhang's root). The edge beam considered was 400x400 mm^2 and was added at the free edge of the slab without edge beam (**Figure 13**). The top and the middle, and the bottom longitudinal reinforcement in the edge beam consists of ⌀16 mm and ⌀20 mm bars respectively. The transversal reinforcement is ⌀10 mm every 300 mm.

Material properties and models

The mechanical properties based on the experimental test are presented in **Table 1**. In the FE-models the properties corresponding to test DR1a for concrete were used for all the simulations. The rationale is that a fair comparison between different loading situations was pursued in this work. This also enabled an impartial assessment of the calculation methods. The authors would still like to remark that the consideration of the properties described for the other tests led to almost negligible differences in the structural response. The material model chosen for concrete was 'Concrete Damaged Plasticity', which was proposed by Lubliner, Oliver, Oller, & Onate (1989) and modified by Lee & Fenves (1998). The values of the parameters are shown in **Table 2**. The tensile behavior was defined according to the model presented by Cornelissen, Hordijk, & Reinhardt (1986), which is considered the most accurate for tensile cracking (Karihaloo, 2003). Concerning the compressive behavior, the guidance of the Eurocode 2 (CEN, 2005) adapted to the biaxial compression curves presented in the experimental test was used. The material model chosen for the reinforcement is 'Plastic' which allows defining a plastic isotropic hardening after yielding (**Table 2**).
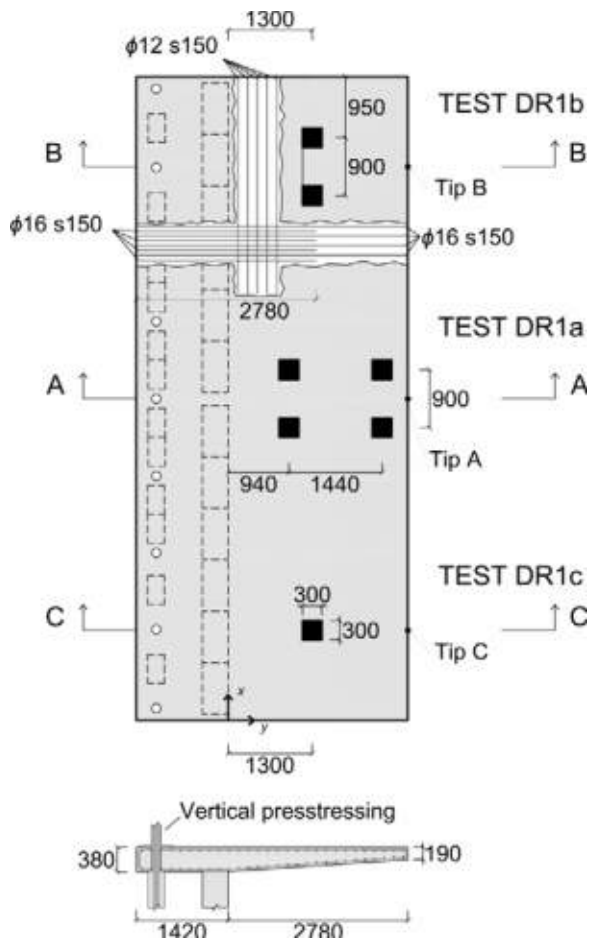
Figure 12: Geometry and reinforcement of the experimental tests. Adapted from Vaz Rodrigues R. (2007)
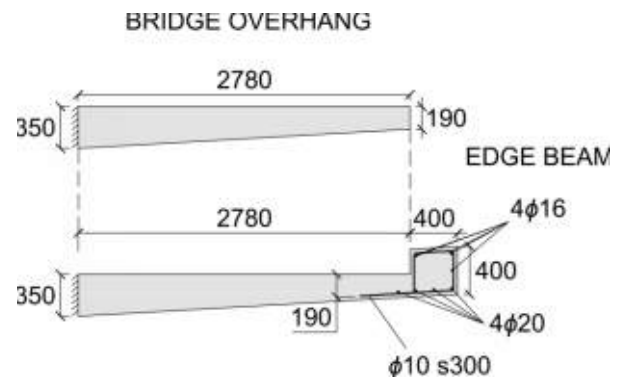

Figure 13: Overhang bridge slab without and with an edge beam including the reinforcement

Table 1: Mechanical properties of the concrete in the experimental test

Test	Parameter	Symbol	Unit	Value
All	Density	ρ_c	kg/m^3	2450
	Poisson ratio	ν_c	-	0,2
	Dilation angle	φ	-	35
	Flow-potential eccentricity	e	-	0,1
	Ratio biaxial–uniaxial compression	f_{b0}/f_{c0}	-	1,16
	Second tensile-compressive stress invariant ratio	K	-	0,667
	Viscosity parameter	μ	-	1E-10
DR1a	Compressive strength	f_{cc}	MPa	39,11
	Tensile strength	f_{ct}	MPa	2,94
	Young's modulus	E_c	GPa	36,03
DR1b	Compressive strength	f_{cc}	MPa	39,91
	Tensile strength	f_{ct}	MPa	3,02
	Young's modulus	E_c	GPa	36,09
DR1c	Compressive strength	f_{cc}	MPa	40,82
	Tensile strength	f_{ct}	MPa	3,11
	Young's modulus	E_c	GPa	36,16

Table 2: Mechanical properties of the reinforcement

Bar diameter	Parameter	Symbol	Unit	Value
All	Density	ρ_s	kg/m^3	7800
	Young modulus	E_s	GPa	200
	Poisson ratio	ν_s	-	0,3
Ø16 mm Ø20 mm	Yield strength	f_y	MPa	499
	Tensile strength	f_t	MPa	600
	Deformation under maximum load	ε_u	(%)	10,73
Ø12 mm Ø10 mm	Yield strength	f_y	MPa	541
	Tensile strength	f_t	MPa	629
	Deformation under maximum load	ε_u	(%)	9,05

Mesh size and non-linear analysis procedure

For the linear analyses a 50 mm mesh has been used formed by 4-noded shell quadrilateral elements. For the non-linear analyses, an approx. 25 mm mesh formed by 8-noded solid hexahedral elements was used for concrete. This enabled at eleven elements across the height of the slab which is suitable to describe shear behavior. A 25 mm mesh formed by truss elements was used for the reinforcement. The task was considered non-linear because of a brittle shear failure which led to the performance of a quasi-static analysis to prevent convergence issues. The loading step was smoothed to avoid inertial forces affecting the results. The total and kinetic energy of the model during the simulation were monitored to control this effect.

Loading, boundary conditions and constraints

A statically-determined load-structure built of beams and trusses was connected through a constraint equation to the loading plates, which were simultaneously connected to the reinforced concrete overhang. Such structure was used to ensure better convergence and the possibility to reflect more accurately the load-displacement curves (Broo, Lundgren, & Plos, 2008). A prescribed displacement-control was assigned to a node on top of the load-structure to appreciate vertical fluctuations of the total force applied. The reaction force was calculated subsequently. The support of the column is represented by restraining all the degrees of freedom of the bottom surface. The prestressing was modelled by restraining all the degrees of freedom at the two contact surfaces of the slab. Fully bonded reinforcement was used forcing the nodes of the bars to follow the displacement degrees of freedom of the surrounding concrete.

3.2 MODEL VALIDATION

A comparison between the load-displacement curves and a cut failure surface from the tests and the non-linear FE-model is shown in **Figure 14**. The total load represented refers to the sum of all the applied loads in each test. The displacement corresponds to the tip of the cantilever located at the symmetry axis with respect to the load application for each test, as depicted in **Figure 12**. The difference in the beginning of the curve of test DR1 is justified by the initial cyclic loading performed. A shear failure mode was observed for all the FE-models, in agreement with the experimental tests. The results obtained for tests DR1b and DR1c show a stiffer response than that of the experiment. The authors believe that this fact is motivated by the manner the experiment was performed where the tests were carried out successively in the following order: DR1a, DR1b and DR1c. A consideration of this aspect would lead to a less stiff behavior. Furthermore, the load history was not accounted for, which would also affect the initial stiffness. Numerical simulations using damage parameters that can account for these aspects are underway. In this work, nonetheless, it is of interest to study the behavior of the slab without any previous loading history that can have an influence. The results presented were considered accurate enough to validate the FE-model for its application in the case of

the addition of an edge beam. The authors believe that a reasonable match between the load-displacement curves was obtained.
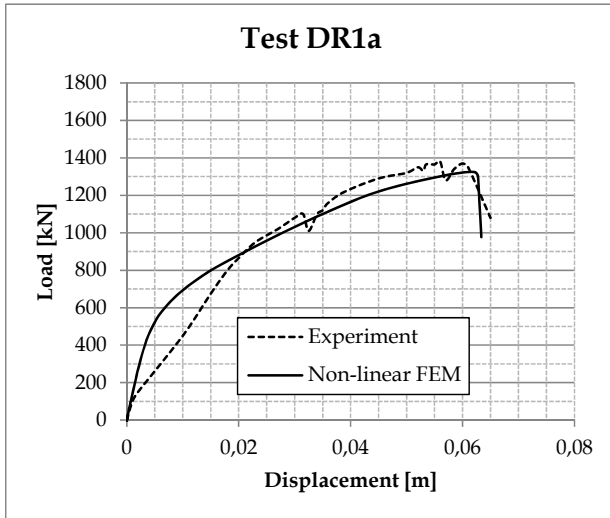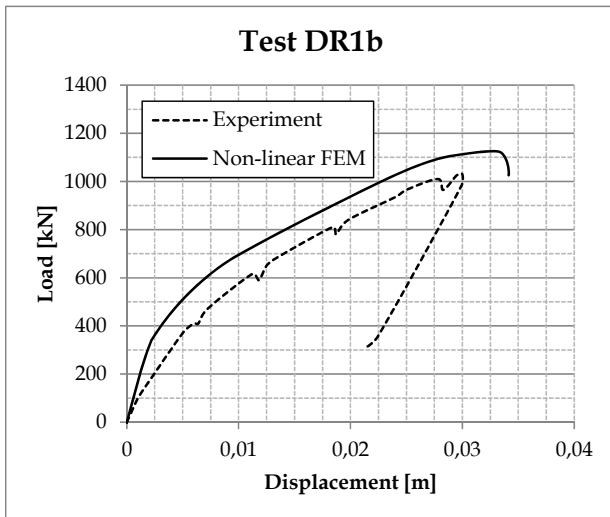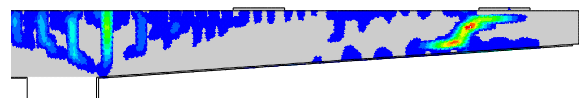

$$\frac{Q_{\text{nlFE,DR1a}}}{Q_{\text{exp,DR1a}}} = \frac{1325}{1397} = 0,95$$

Experimental test:

Non-linear FE-model:

$$\frac{Q_{\text{nlFE,DR1b}}}{Q_{\text{exp,DR1b}}} = \frac{1125}{1025} = 1,09$$
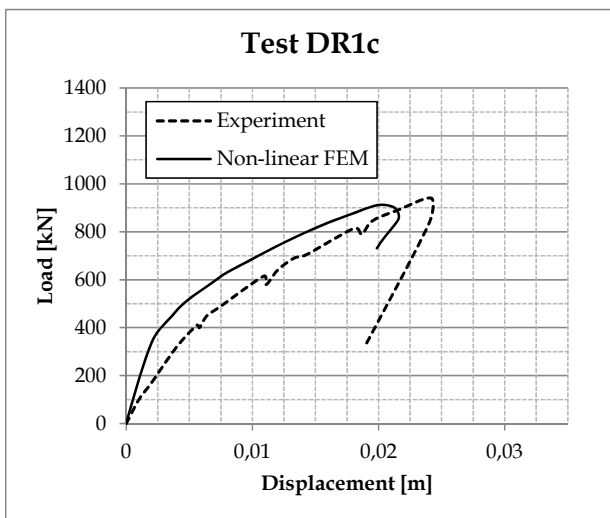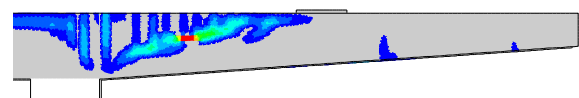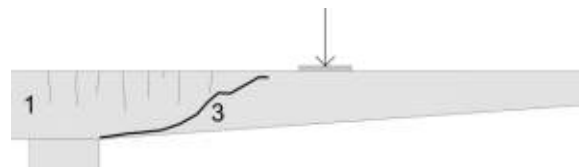
Experimental test:
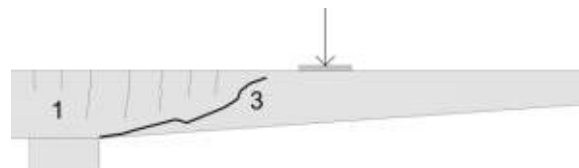
Non-linear FE-model:

$$\frac{Q_{\text{nlFE,DR1c}}}{Q_{\text{exp,DR1c}}} = \frac{912}{910} = 1,00$$

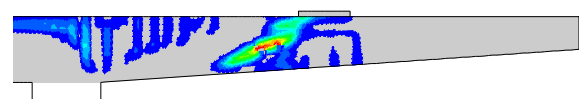Experimental test:

Non-linear FE-model:

Figure 14: Load-displacement curves and failure surfaces after cutting of the slabs obtained from the experimental tests and the non-linear FE-models for tests DR1a, DR1b and DR1c

4. RESULTS AND DISCUSSION

The results in this chapter are presented in the following order: simplified hand calculations, linear-elastic FE-analysis and non-linear FE-analysis. The bending critical cross section is located at the root of the cantilever. The shear critical cross sections considered for bending and shear for tests DR1, DR1b and DR1c are located at a distance $d/2$ from the load application point (**Figure 15**). Two critical cross sections have been considered for test DR1a corresponding to each load position (CSI and CSII). These critical cross sections are the same for both cases without and with an edge beam. Safety coefficients were not used to capture the real behavior according to the experimental tests.
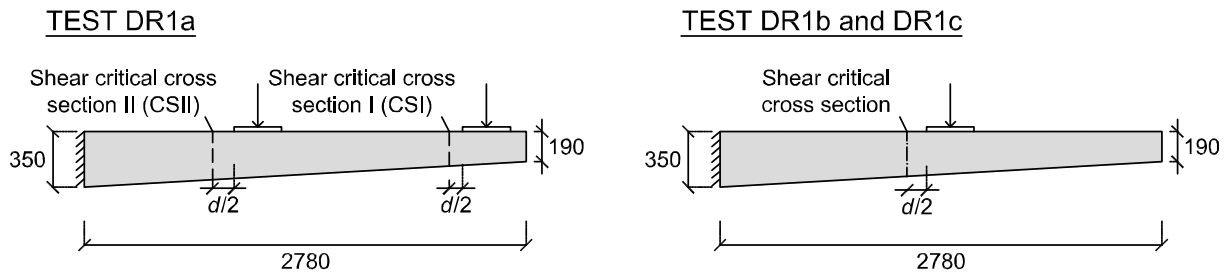

Figure 15: Shear critical cross sections considered for experimental tests DR1a, DR1b and DR1c.

4.1 SIMPLIFIED CALCULATIONS

Shear forces

The load capacity (Q_{Rd}) due to shear forces using the guidelines provided by Eurocode 2 and BBK94 is presented in **Table 3**. The distribution widths (w_{B11}) from the guidance provided by Bro 11 were used. An underestimation of the load capacity of RC overhang slab for the cases with an edge beam was documented. The rationale is that this approach only considers the added self-weight and does not account for any positive influence of such member. A positive influence of the edge beam is not reflected on the distribution widths either. A considerable difference of around 60% between BBK94 and Eurocode is observed. This fact is further discussed in **Section 4.4**, including also a comparison to the experimental results.

Table 3: Shear load capacity according to Bro 11 ($Q_{\mathrm{Rd,B11}}$) and BBK94 ($Q_{\mathrm{Rd,BBK}}$)

	$v_{\mathrm{Rd,B11}}$ [kN/m]	$v_{\mathrm{Rd,BBK}}$ [kN/m]	w_{B11} [mm]		$Q_{\mathrm{Rd,B11}}$ [kN]			$Q_{\mathrm{Rd,BBK}}$ [kN]			$\dfrac{Q_{\mathrm{BBK,Rd}}}{Q_{\mathrm{B11,Rd}}}$	
Test			nEB	EB	nEB	EB	nEB/EB	nEB	EB	nEB/EB	nEB	EB
DR1a CS-I	193	294	2917	2917	1060	1037	1,02	1651	1628	1,02	1,56	1,56
DR1a CS-II	306	474	3965	3965	1195	1179	1,01	1859	1844	1,01	1,56	1,56
DR1b	294	453	3703	3703	1047	1032	1,01	1637	1622	1,01	1,60	1,60
DR1c	294	453	2803	2803	776	764	1,01	1222	1211	1,01	1,65	1,65

nEB: without edge beam; EB: with edge beam

In the previous calculations the favorable influence of the tapered thickness was not accounted for. For a hand-calculation of a slab such effect is not straight forward to consider since the distribution of moments is not uniform. To assess its influence, the maximum bending moment at the critical cross section in the direction perpendicular to the root of the overhang obtained from a linear-elastic FE-analysis was used. It has to be noted that this approach may result unsafe because it may overestimate the shear capacity. In reality, if the principal shear force is distributed then a distributed moment should be considered as well, accounting for the directions of the principal shear at each loca-

tion. **Table 4** visualizes the difference of taking into consideration such effect following the guidance of BBK94 ($Q_{\mathrm{Rd,BBKi}}$).

Table 4: Influence of the consideration of the inclined compression chord using BBK94 on the shear load capacity ($Q_{\mathrm{Rd,BBK}}$ and $Q_{\mathrm{Rd,BBKi}}$)

	$v_{\mathrm{Rd,BBK}}$ [kN/m]	$v_{\mathrm{Rd,BBKi}}$ [kN/m]	$w_{\mathrm{s,B11}}$ [mm]		$Q_{\mathrm{Rd,BBK}}$ [kN]			$Q_{\mathrm{Rd,BBKi}}$ [kN]			$\dfrac{Q_{\mathrm{BBK,Rd}}}{Q_{\mathrm{BBKi,Rd}}}$	
Test			nEB	EB	nEB	EB	nEB /EB	nEB	EB	nEB /EB	nEB	EB
DR1a CS-I	294	303	2917	2917	1651	1628	1,02	1702	1678	1,01	1,03	1,03
DR1a CS-II	474	542	3965	3965	1859	1844	1,01	2132	2116	1,01	1,15	1,15
DR1b	453	478	3703	3703	1637	1622	1,01	1728	1713	1,01	1,06	1,06
DR1c	453	475	2803	2803	1222	1211	1,01	1285	1274	1,01	1,05	1,05

nEB: without edge beam; EB: with edge beam

The consideration of the influence of a tapered bottom thickness may be considered negligible (3-6%) for one or more concentrated loads applied in a single row parallel to the root. In contrast, it becomes more pronounced (15%) for the case of four concentrated applied loads for critical section II (two rows of forces parallel to the root). The rationale is that the bending moment calculated at this location is of a higher magnitude because it accounts for all the loads applied. The authors conclude that the addition of this contribution should be handled with care as it may lead to unsafe estimates.

Bending moments

The lower-bound flexural load capacity using the simplified method of Homberg & Ropers (1965) denoted as $Q_{\mathrm{Rd,HR}}$ is presented in **Table 5.** An extension of the concrete deck slab with an equivalent flexural rigidity to the edge beam was considered. The presence of an edge beam leads to a higher resisting moment capacity and thus a higher load capacity, especially for the case of four concentrated loads. The theoretical lower-bound flexural failure load is slightly lower than the shear failure $Q_{\mathrm{Rd,B11}}$ which indicates that either flexion or shear could be not critical for the design of the bridge overhang. This is in agreement with the tests as pronounced yielding in the flexural reinforcement was documented. If $Q_{\mathrm{Rd,BBK}}$ was considered instead, the design flexural load would be critical. This fact might explain in some part the lack of robustness in those bridges as the designers believed that a ductile flexural failure would be the critical one.

Table 5: Flexural load capacity using Homerg&Ropers influence surfaces ($Q_{\mathrm{Rd,HR}}$)

	$Q_{\mathrm{Rd,HR}}$ [kN]		
Test	nEB	EB	nEB /EB
DR1a	1046	1250	0,84
DR1b	1173	1301	0,90
DR1c	966	1084	0,89

nEB: without edge beam; EB: with edge beam

4.2 LINEAR-ELASTIC FE-ANALYSIS

Shear forces

Table 6 presents the shear load capacity for a linear-elastic FE-analysis ($Q_{\mathrm{Rd,lFE}}$). The distributed principal shear force ($v_{\mathrm{lFE,d}}$) using the recommendations provided by Pacoste et. al. (2012) and the shear resisting capacity for each critical cross-section (v_{Rd}) are also presented. **Figure 16** illustrates

the distribution of the principal shear force per unit width v_0 in the corresponding critical cross sections for tests DR1a, DR1b and DR1c for $Q_{\mathrm{Rd,lFE}}$.

Even though the presence of an edge beam is not clearly distinguished by the formulae to late $w_{\mathrm{s,PPJ}}$, an interesting fact to highlight is the change of the shear flow direction because of such member, which influences the use of the limitation presented in **Figure 11**. For slab DR1a without an edge beam at the critical cross section I, such limitation had to be used. This was not the case with an edge beam. The rationale is that the shear stream lines become more perpendicular to the support which deactivates such limitation. The load is transferred in the longitudinal direction which contributes to a wider distribution of the shear forces. As a result, $Q_{\mathrm{Rd,lFE}}$ for test DR1a is considerably augmented in the case of an edge beam.

Another interesting fact is that with an edge beam, cross section II becomes the critical one for design, which was by far not the case without an edge beam. These facts confirm a 'stiffening effect' of the edge beam for loads applied close to the free edge, which is related to its load-carrying function. Still, cross section I lies very close to its maximum shear resistance capacity. This can be interpreted as an efficient distribution of the shear resisting capacity of the bridge overhang, which does not occur without an edge beam. Concerning tests DR1b and DR1c the presence of the edge beam can be considered negligible, which is motivated by the fact that the loads are not close to the free edge. A comparison between the load capacity calculated using the maximum principal shear force ($Q_{\mathrm{lFE,max}}$) and the distributed shear force ($Q_{\mathrm{lFE,d}}$) is presented in **Table 7**. The choice of the maximum principal shear force ($v_{\mathrm{lFE,max}}$) without redistribution as the design value is shown to be very conservative, especially for only one and two concentrated loads.
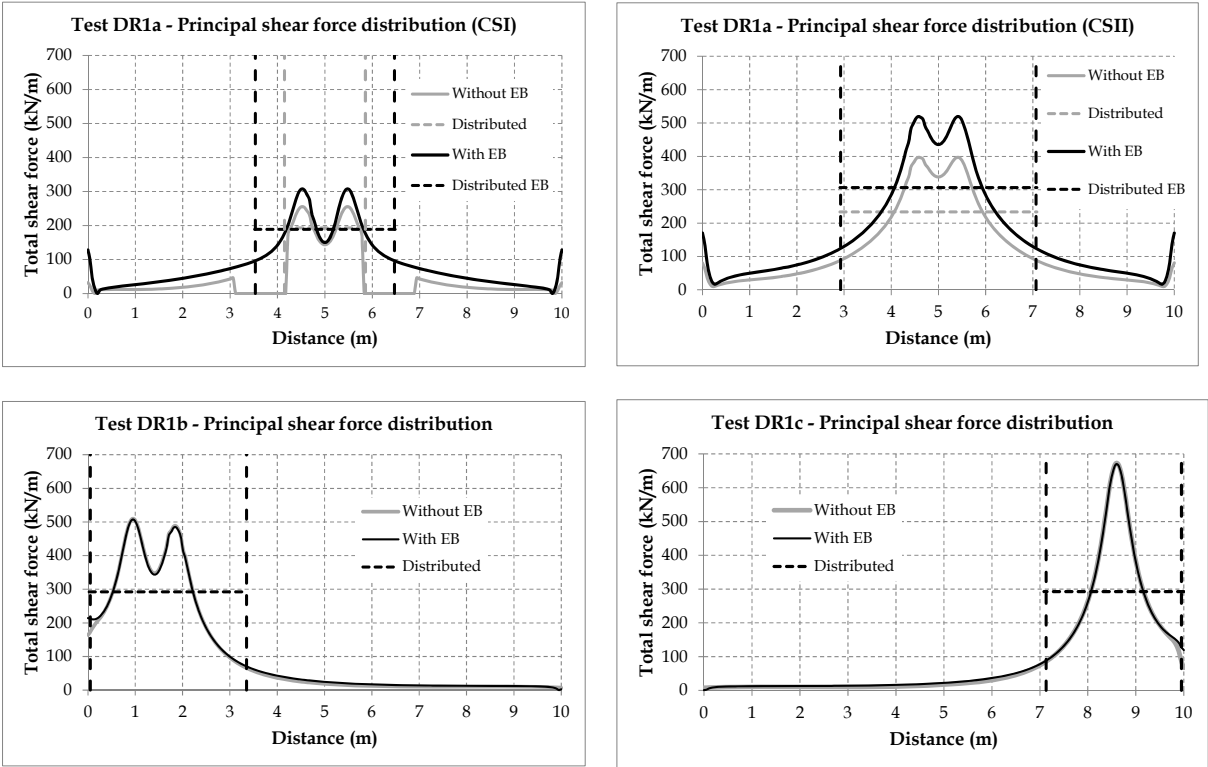

Figure 16: Principal shear force along the critical cross section and corresponding distribution width according to Pacoste et. al. (2012) for tests DR1a, DR1b and DR1c.

Table 6: Shear load capacity obtained from a linear-elastic FE-analysis for tests DR1a, DR1b and DR1c

Test	$w_{\mathrm{s,PPJ}}$ [mm]		$v_{\mathrm{Rd,CSI}}$	$v_{\mathrm{Rd,CSII}}$	$v_{\mathrm{lFEd,CSI}}$	$v_{\mathrm{lFEd,CSII}}$	$Q_{\mathrm{Rd,lFEd}}$ [kN]		
	nEB	EB	nEB	EB	nEB	EB	nEB	EB	~~EB~~/EB
DR1a – CS I	1709	2937	193	306	**193**	233	986	1362	0,72
DR1a – CS II	4142	4142	193	306	189	**306**	986	1362	0,72
DR1b	3370	3370	296	296	296	296	951	953	1,00
DR1c	2890	2890	298	298	298	298	802	804	1,00

nEB: without edge beam; EB: with edge beam

Table 7: Comparison of the load capacity obtained from the maximum and the distributed shear force

Test	$Q_{\mathrm{Rd,lFEd}}$ [kN]		$Q_{\mathrm{Rd,lFEmax}}$ [kN]		$\dfrac{Q_{\mathrm{Rd,lFEd}}}{Q_{\mathrm{Rd,lFEmax}}}$	
	nEB	EB	nEB	EB	nEB	EB
DR1a	986	1362	765	777	1,29	1,75
DR1b	951	953	541	542	1,75	1,76
DR1c	802	804	344	346	2,32	2,33

nEB: without edge beam; EB: with edge beam

Bending moment

The flexural load capacity ($Q_{\mathrm{Rd,mlFEd}}$) for the tests with and without edge beam calculated from a linear-elastic FE-analysis following the recommendations proposed by Pacoste et. al. (2012) is presented in **Table 8.** The distribution of m_{y} for $Q_{\mathrm{Rd,mlFEd}}$ is presented in **Figure 17**. To calculate $w_{\mathrm{m,PPJ}}$ the second formula in **Eq. 4** had to be used because the ratio x_{u}/d was 0,13. The flexural load capacity is higher compared to the ones obtained from the shear capacity for experimental tests DR1b and DR1c. For the case of test DR1a a slight difference is appreciated, partly because the method used is lower bound and, hence, conservative. However, it is important to remark that considerable yielding of the flexural reinforcement was observed in this case.

The presence of an edge beam has a slight relevance for test DR1a. A smooth reduction in m_{y} at the cantilever's root exists for the case of four concentrated loads, in agreement with the results presented by Vaz Rodrigues R. (2007). The FE-model accounts for the presence of the edge beam for the moment distribution, in contrast with the simplified calculation methods. Such positive effect should be handled with care. Duran (2014) showed that m_{y} can become even higher for the case with an edge beam. The cantilever span a and the size of the edge beam would be the governing factors controlling such effect. For tests DR1b and DR1c where the loads are closer to the overhang's root such effect can be considered negligible.
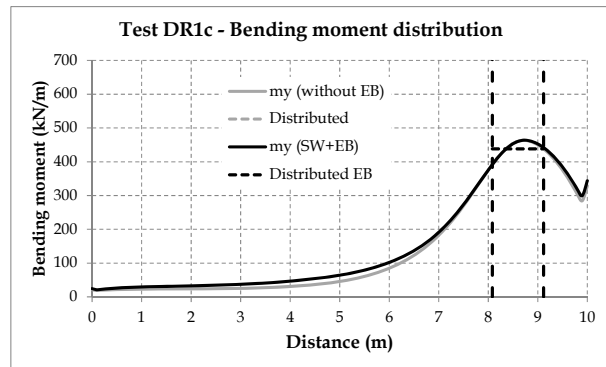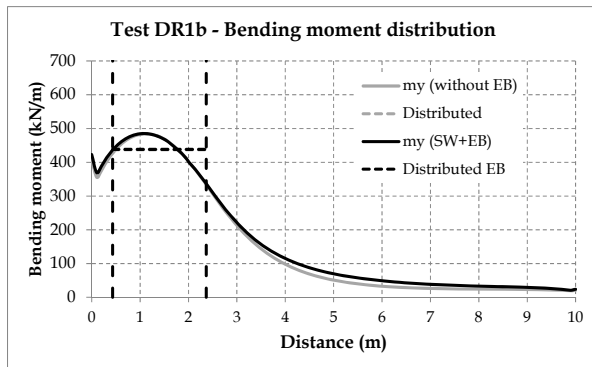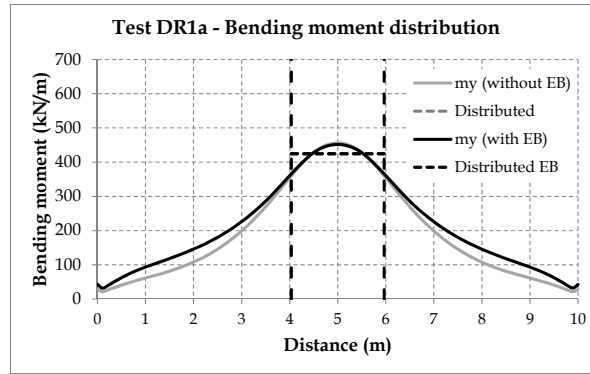
Figure 17: Distribution of m_y in the cantilever root for and corresponding distribution widths according to Pacoste, et. al. (2012) for $Q_{Rd,mFE}$ for tests DR1a, DR1b and DR1c

Table 8: Flexural load capacity for linear-elastic FE-analysis

	$w_{m,PPJ}$ [mm]		$m_{y,Rd}$ [kN/m]		$m_{d,distr}$ [kN/m]		$Q_{Rd,mlFEd}$ [kN]		
Test	nEB	EB	nEB	EB	nEB	EB	nEB	EB	nEB /EB
DR1a – Section I	1934	1934	438		438		1040	1121	0,93
DR1b	1934	1934	438		438		1043	1055	0,99
DR1c	1034	1034	438		438		926	939	0,99

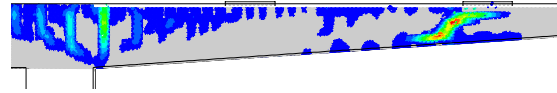nEB: without edge beam; EB: with edge beam

4.3 NON-LINEAR FE-ANALYSIS

Figure 18 shows the load-displacement curves and the failure modes obtained from the non-linear analysis for the case with and without edge beam for test configurations DR1a, DR1b and DR1c. A higher load capacity of the bridge overhang was observed because of the presence of the edge beam, more substantially in test DR1a (15%). A shear failure mode was also observed. The failure surface did not extend through the edge beam, resembling a punching failure, in consonance with the findings of Lu (2003). A secondary crack developing in the critical cross section II may become significant and the slab can even fail at that point, in agreement with experimental results and the simplified methods. This fact proves the efficient distribution of shear forces for the case with an edge beam. The load capacity is barely increased for the tests DR1b and DR1c. A slight increased ductility was observed in test DR1a with an edge beam, whereas a more fragile failure occurs in tests DR1b and DR1c.
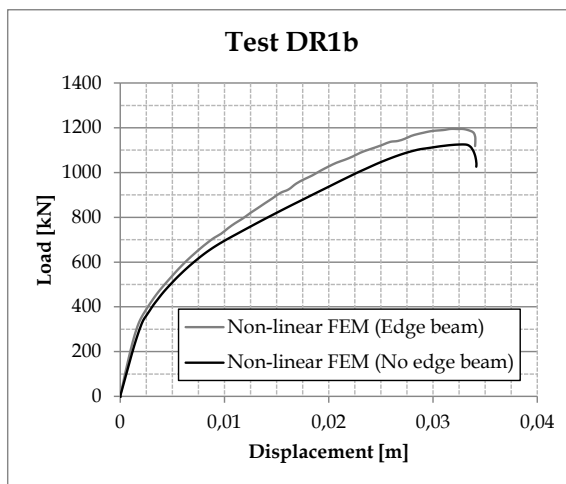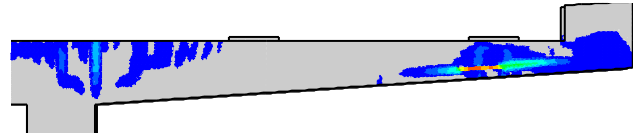
Test DR1a
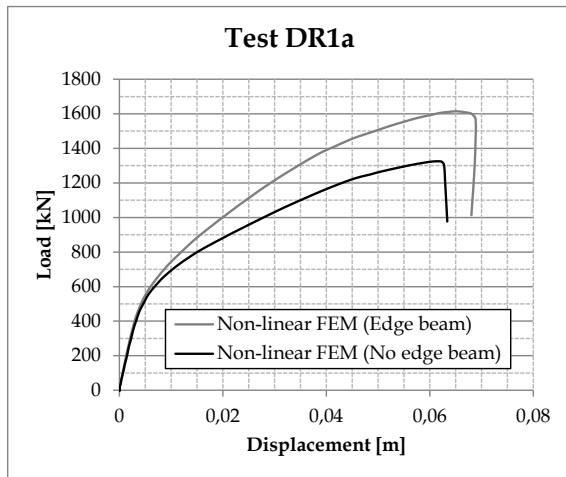
$$\frac{Q_{\mathrm{nlFE,DR1aEB}}}{Q_{\mathrm{nlFE,DR1a}}} = \frac{1614}{1325} = 1,22$$

FE-model without edge beam:

FE-model with edge beam:

Test DR1b

$$\frac{Q_{\mathrm{nlFE,DR1bEB}}}{Q_{\mathrm{nlFE,DR1b}}} = \frac{1195}{1125} = 1,06$$

FE-model without edge beam:

FE-model with edge beam:

Test DR1c
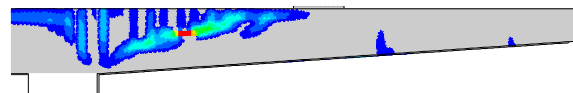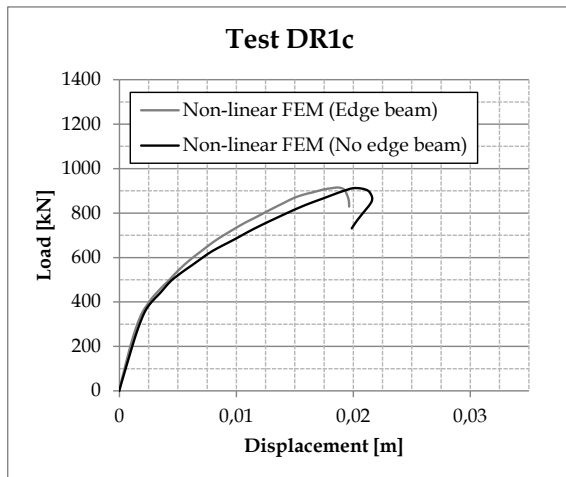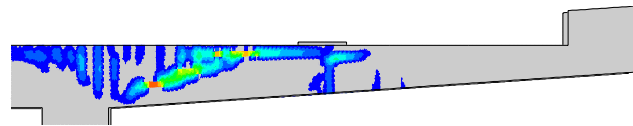
$$\frac{Q_{\mathrm{nlFE,DR1cEB}}}{Q_{\mathrm{nlFE,DR1c}}} = \frac{914}{912} = 1,00$$

FE-model without edge beam:
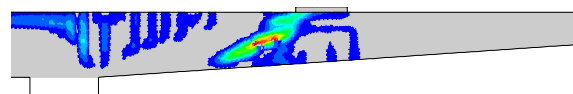
FE-model with edge beam:
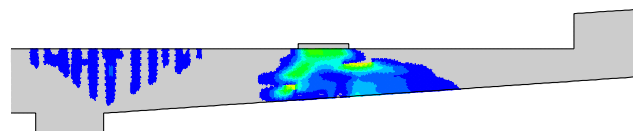
Figure 18: Load-displacement curves and failure surfaces after cutting of the slabs obtained from a non-linear analysis for tests DR1a, DR1b and DR1c with and without edge beam

4.4 ANALYSIS OF THE LOAD CAPACITY

Table 9 and **Table 10** gathers all the load capacities presented in the previous sections for shear and bending respectively. A comparison to a reference load capacity (Q_{ref}) is visualized. The Q_{ref} chosen for the results of the bridge overhang without edge beam refers to the one from the experimental

tests (Q_{exp}). For the case with the edge beam, since there was no experimental data, the one obtained from the validated non-linear FE-model (Q_{nlFE}) has been elected. Results obtained from a punching criterion using the 3-sided control perimeters $2d$ and $d/2$ are also included.

Table 9: Summary of shear load resisting capacities obtained through different methods and comparison to the experimental tests and the non-linear FE-model

	Test DR1a				Test DR1b				Test DR1c			
	Without EB		With EB		Without EB		With EB		Without EB		With EB	
	Q [kN]	$\dfrac{Q}{Q_{ref}}$	Q [kN]	$\dfrac{Q}{Q_{ref}}$	Q [kN]	$\dfrac{Q}{Q_{ref}}$	Q [kN]	$\dfrac{Q}{Q_{ref}}$	Q [kN]	$\dfrac{Q}{Q_{ref}}$	Q [kN]	$\dfrac{Q}{Q_{ref}}$
Q_{ref}	**1397**		**1614**		**1025**		**1195**		**910**		**914**	
$Q_{Rd,nlFE}$	1325	0,95	1614	1,00	1125	1,10	1195	1,00	912	1,00	914	1,00
$Q_{Rd,B11}$	1060	0,76	1037	0,64	1047	1,02	1032	0,86	787	0,87	776	0,85
$Q_{Rd,BBK}$	1651	1,18	1628	1,01	1637	1,60	1622	1,36	1222	1,34	1211	1,33
$Q_{Rd,BBKi}$	1702	1,22	1678	1,04	1728	1,69	1713	1,43	1285	1,41	1274	1,39
$Q_{Rd,lFEd}$	986	0,71	1362	0,84	949	0,93	951	0,80	798	0,88	800	0,88
$Q_{Rd,lFEmax}$	765	0,55	777	0,48	542	0,53	541	0,45	344	0,38	344	0,38
$Q_{Rd,pun,d/2}$	565	0,40	552	0,34	555	0,54	547	0,46	355	0,39	350	0,38
$Q_{Rd,pun,2d}$	849	0,61	830	0,51	990	0,97	860	0,72	668	0,73	658	0,72

Table 10: Summary of bending load resisting capacities obtained through different methods and comparison to the experimental tests and the non-linear FE-model

	Test DR1a				Test DR1b				Test DR1c			
	Without EB		With EB		Without EB		With EB		Without EB		With EB	
	Q [kN]	$\dfrac{Q}{Q_{ref}}$	Q [kN]	$\dfrac{Q}{Q_{ref}}$	Q [kN]	$\dfrac{Q}{Q_{ref}}$	Q [kN]	$\dfrac{Q}{Q_{ref}}$	Q [kN]	$\dfrac{Q}{Q_{ref}}$	Q [kN]	$\dfrac{Q}{Q_{ref}}$
Q_{ref}	**1397**		**1614**		**1025**		**1195**		**910**		**914**	
$Q_{Rd,HR}$	1046	0,75	1251	0,77	1173	1,15	1301	1,09	966	1,06	1084	1,19
$Q_{Rd,mlFEd}$	1040	0,74	1121	0,69	1043	1,02	1055	0,88	926	1,02	939	1,03
$Q_{Rd,mlFEmax}$	998	0,71	1082	0,67	937	0,92	948	0,79	874	0,96	885	0,97

The results obtained using the existing Swedish regulations Bro 11 following the Eurocode may be considered adequate for the case without an edge beam, but conservative for the case with an edge beam. In contrast, the use of BBK94 may lead to an overestimation of the bridge load resisting capacity for shear, which is more accentuated if the positive compression chord contribution is accounted for. This would motivate the increased use of more shear reinforcement (stirrups) in recent bridges that were designed according to Eurocode compared to the ones designed using BBK94. Moreover, the results may be interpreted as a lack of sufficient robustness, which has been documented in Swedish bridges. A design performed from a punching perspective using the control perimeter at a distance $2d$ leads to a very conservative estimate of the total load resisting capacity. A much better agreement is achieved if a distance of $d/2$ is contemplated.

Concerning the results from the linear-elastic FE-model, the recommendations provided by Pacoste, et. al. (2012) are reasonable and provide a good match according to the experimental tests and the

non-linear FE-model for both cases with and without an edge beam. The use of the maximum value as the design one is shown to be very conservative.

The flexural failure load calculated is not critical compared to shear failure load, except for the design according to BBK94. It is important to notice that a bending failure would become dominant for larger overhang spans or larger edge beams.

The presence of the edge beam should be especially considered for concentrated loads close to the transversal free edge of the bridge overhang. The edge beam functions as a load-carrying member and provides a wider distribution of shear forces. The removal of the edge beam would imply less loading capacity and thus less robustness in the bridge overhang compared to existing bridges with an edge beam. This fact might result in an increase of the thickness in a critical cross section for a concentrated load close to the transversal free edge, or the use of transversal reinforcement, if the same load capacity of the RC bridge overhang slab with the edge beam is desired.

5. CONCLUSIONS AND FURTHER RESEARCH

Bridge cantilevers are a sensitive part of the bridge deck because they must resist simultaneously high moments and shear forces induced by concentrated loads. The influence of an edge beam on the structural behavior of a RC bridge overhangs has been investigated. Different design methodologies have been compared to experimental tests and a validated non-linear FE-model, and their suitability has been discussed. The following conclusions are drawn:

- The presence of an edge beam increases the load capacity of RC slabs of bridge overhangs for loads placed near the free edge. This 'stiffening effect' is associated with the edge beam's load-carrying function. The edge beam influences considerably the distribution of shear forces near the free edge. A positive influence on the moment distribution would depend on the size of the edge beam and the length of the overhang. The influence of the edge beam for loads applied near the overhang root is almost negligible.

- The aforementioned 'stiffening effect' may imply that the critical cross section governing the design changes for the case of concentrated loads near the free edge in a RC slab with an edge beam. In this case, both critical cross sections close the overhang root and the free edge can be critical for the design. This fact can be interpreted as an efficient distribution of the shear resisting capacity of the RC overhang slab.

- Consequently, if compared with existing road bridges, the removal of the edge beam would imply loss of robustness. Thus, in order to increase the load capacity of the RC bridge overhang slab, an alternative could be to increase the depth of the cross section closest to the transversal free edge. Another alternative, which might not be desired by contractors because of the additional expenses, would be to add stirrups.

- Even though quite conservative estimates are obtained for simple hand calculations, these methods can be considered useful in conception and control of the results obtained with a FE-analysis. The distribution widths according to the Swedish code used together with the Eurocode are quite conservative for the case of an edge beam. If a puching problem is considered, the use of a control perimeter at a distance $2d$ leads to reasonable results. In contrast, if a distance of $d/2$ is used, very conservative results are obtained.

- The old Swedish code BBK94 (Boverket, 1994) may overpredict the shear load capacity of the RC bridge overhang, which could explain the lack of sufficient robustness of Swedish bridges. This fact is accentuated if a positive influence of a variable depth is considered. Unsafe results may be obtained. In contrast, the Eurocode provides conservative estimates. The influence of the edge beam should be accounted for in the existing design regulations for loads applied near the free edge.

- The choice of the maximum shear force and bending moment obtained from the FE-model as the design values is very conservative. The results obtained using the distribution widths proposed by Pacoste et. al. (2012) are considered very adequate, even for the cases with an edge beam, where the limitation specified considering the direction of the principal shear flow applies.

- Non-linear FE-analyses with continuum elements can simulate in an acceptable manner the shear failure of RC slabs of bridge overhangs without stirrups. The load capacity and the displacement can be obtained. An explicit solver where the load is applied in a quasi-static manner can be used to prevent convergence issues.

Future research by the authors will involve, among other things, the influence of different thicknesses and slopes, and the reinforcement ratio in the bridge overhang, considering dimensions from Swedish bridges. An investigation of different failure modes depending on the geometry of the bridge overhang, the thickness of the slab and the size of the edge beam is also of interest. Modelling a vehicle crash for a case without the edge beam for the development of a solution of an edge beam is also under consideration.

Bibliography

ACI [American Concrete Institute]. (2014). *318-14: Building Code Requirements for Structural Concrete and Commentary.* Farmington Hills, Michigan: ACI.

Bakht, B. (1981). Simplified Analysis of Edge Stiffened Cantilever Slabs. *Journal of the Structural Division*, 535-550.

Bakht, B., & Holland, D. (1976). A manual method for the elastic analysis of wide cantilever slabs of linearly varying thickness. *Canadian Journal of Civil Engineering, Vol. 3 (4)*, pp. 523-530.

Boverket. (1994). *Betongkonstruktioner [Concrete design].* Boverket.

Broo, H., Lundgren, K., & Plos, M. (2008). *A guide to non-linear finite element modelling of shear and torsion in concrete bridges.* Gothemburg: Chalmers University of Technology.

Canadian Standards Association. (2015). *CAN/CSA-S6 Canadian Highway Bridge Design.* Missisauga, Ontario: Canadian Standards Association.

Cornelissen, H., Hordijk, D., & Reinhardt, H. (1986). *Experimental determination of crack softening characteristics of normal weight and lightweight concrete* (Vol. Vol. 31 No. 2). (Heron, Ed.) Delft: Delft University of Technology.

Dilger, W. H., Tadros, G., & Chebib, J. (1990). Bending moments in cantilever slabs. *Development in Short and Medium Span Bridges '90, Vol. 1*, pp. 265-276.

Duran, E. (2014). *Design of edge beams.* Stockholm: KTH Royal Institute of Technology. Retrieved from http://www.diva-portal.org/smash/get/diva2:732710/FULLTEXT01.pdf

European Committee for Standardization [CEN]. (2005). *Eurocode 2: Design of concrete structures - Part 1-1: General rules and rules for buildings. EN 1992-1-1.*

Hedman, O., & Losberg, A. (1976). *Skjuvhållfasthet hos tunna betongplattor belastade med rörliga punktlaster. Preliminär delrapport till Vägverket maj 1976.* Stockholm.

Homberg, H., & Ropers, W. (1965). *Farhrbahnplatten mit veränderlicher Dicke; Erster Band.* Springer-Verlag.

Ibell, T., & Morley, C. M. (1999). Stregth and Behavior in Sehar of Concrete Beam-and-Slab Bridges. *ACI Structural Journal, Vol. 96 No. 3*, 386-392.

Jaramillo, T. (1950, March). Deflections and Moments due to a Concentrated Load on a Cantilever Plate of Infinite Length. *Journal of Applied Mechanics, Vol. 72 No. 1*, p. A-67 to A-72.

Karihaloo, B. (2003). Failure of concrete. In *Comprenhensive Structural Integrity* (Vol. Vol. 2.10, pp. 475-546).

Kelindeman, M. (2014). *Edge Beams. Evaluation of Investment Costs for its application to LCC Analysis.* Master Thesis, KTH Royal Institute of Technology, Stockholm.

Lee, J., & Fenves, G. (1998). Plastic-Damage Model for Cycli Loading of Concrete Structures. *Journal of Engineering Mechanics, Vol. 124, No. 8*, 892-900.

Lim, S. (2013). *Redistribution of force concentrations in reinforced concrete cantilever slab using 3D non-linear FE analyses.* Master Thesis, Chalmers University of Technology, Göteborg.

Lu, H.-Y. (2003). *Behaviour of reinforced concrete cantilevers under concentrated loads.* PhD Thesis, University of Cambridge, Girton College.

Lubliner, J., Oliver, J., Oller, S., & Onate, E. (1989). A plastic-damage model for concrete. *International Journal of Solids and Structures, Vol. 25(3)*, 299-329. doi:10.1016/0020-7683(89)90050-4

Miller, R., Aktan, A., & Shahrooz, B. (1994, July). Destructive Testing of Decommissioned Concrete Slab Bridge. *ASCE Journal of Structural Engineering, Vol. 120 No 7*, 2176-2198.

Mufti, A. A., Bakht, B., & Jaeger, L. G. (1993). Moments in deck slabs due to cantilever loads. *Journal of structural engineering New York, N.Y., 119(6)*, 1761-1777.

Muttoni, A. (2008). Punching shear strength of reinforced concrete slabs without transverse reinforcement. *ACI Structural Journal*.

Pacoste, C., Plos, M., & Johansson, M. (2012). *Recommendations for finite element analysis for the design of reinforced concrete slabs.* Stockholm: KTH Royal Institute of Technology, ELU and Chalmers Institute of Technology.

Pettersson, L., & Sundquist, H. (2014). *Optimal Edge Beams: Results of the Research, Development and Demonstration project (Optimala kantbalkssystem: Resultat av genomfört FUD-projekt).* (Technical Report 2014:151). Stockholm: KTH Royal Institute of Technology. Retrieved from DiVA Portal: http://kth.diva-portal.org/smash/record.jsf?pid=diva2%3A761605&dswid=5931

Pucher, A. (1951). *Einflussfelder elastischer Platten.* Wien: Springer Verlag.

Ramos, D. (2015). *Steel edge beam.* Stockholm: KTH Royal Institute of Technology.

Reismann, H., & Cheng, S.-H. (1970). The edge reinforced cantilever plate strip. *IABSE Publications*.

Rombach, G., & Kohl, M. (2013, December). Shear Design of RC Bridge Deck Slabs according to Eurocode 2. *Journal of Bridge Engineering*, 1261-1269. doi:10.1061/(ASCE)BE.1943-5592.0000460

Rombach, G., & Latte, S. (2008). Shear resistance of bridge decks without shear reinforcement. In J. Walraven, & Stoelhorst, D. (Ed.), *Proc., fib Symp.: Tailor Made Concrete Structures* (pp. 519-525). London: Taylor&Francis.

Rombach, G., Kohl, M., & Nghiep, V. (2011). Shear design of concrete members without shear reinforcement - A solved problem? *Proc. 12th East Asia-Pacific Conf. on Structural Engineering and Construction. Vol. 14*, pp. 134-140. Elservier.

Shams Hakimi, P. (2012). *Distribution of Shear Force in Concrete Slabs.* Master Thesis, Chalmers Institute of Technology, Göteborg.

Smith, K. N., & Mikelsteins. (1988). Load distribution in edge stiffened slab and slab-on-girder bridge decks. *I Canadian Journal of Civil Engineering, Vol.15(6)*, pp. 977-983.

Sundquist, H. (2010). *Elastic Plate Theory for Bridge Superstructures.* Stockholm: KTH Royal Institute of Technology.

Sundquist, H. (2011). *Robustare brobaneplatta [More robust bridge decks].* KTH Royal Institute of Technology, Chalmers Institute of Technology and LTH Institute of Technology. Stockholm: Sveriges Bygguniversitet.

Trafikverket [The Swedish Transport Administration]. (2011a). *TRVK Trafikverkets Tekniska Krav Bro 2011:085 [Technical Requirements for Bridges by the Swedish Transport Administration].* Stockholm: Trafikverket. Retrieved from http://publikationswebbutik.vv.se/upload/6500/2011_085_trvk_bro_11.pdf

Trafikverket [The Swedish Transport Administration]. (2011b). *TRVK Trafikverkets Tekniska Råd Bro 2011:086 [Technical Recommendations for Bridges by the Swedish Transport Administration].* Stockholm: Trafikverket. Retrieved from http://online4.ineko.se/online/download.aspx?id=42967

Vaz Rodrigues, R. (2007). *Shear Strength of Reinforced Concrete Bridge Deck Slabs.* École Polytechnique Fédérale de Lausanne.

Vaz Rodrigues, R., Fernández Ruiz, M., & Muttoni, A. (2008). Shear strength of R/C bridge cantilever slabs. *Engineering Structures*, 3024-3033.

Veganzones, J. J., Sundquist, H., Pettersson, L., & Karoumi, R. (2015). Life-cycle Cost Analysis as a tool for the development of bridge edge beams. *Structure and Infrastructure Engineering*.

Wästlund, G. (1964). *Kompendium i Brobyggnad.* Stockholm: KTH Royal Institute of Technology.

Zanuy, C., & Gallego, J. M. (2015). Discussion of Shear Design of RC Bridge Deck Slabs according to Eurocode 2 by Guenter Rombach and Matthias Kohl. *ASCE Journal of Bridge Engineering, Vol. 20*(ISSN 1084-0702), 07014013 1-2.

APPENDIX 1: Nominal shear resistance of concrete members

Eurocode (CEN, 2005)

The nominal shear strength (v_{Rd}) is calculated according to **Eq. 12**. The critical cross section is considered to be at a distance of $2d$ from the load application point. The Swedish code Bro 11 (Trafikverket [The Swedish Transport Administration], 2011b) recommends the use of the Eurocode, even though the use of $d/2$ is advised instead.

$$v_{\mathrm{Rd,EN}} = C_{\mathrm{Rd,c}} \cdot \xi \cdot (100 \cdot \rho_l \cdot f_c)^{1/3} \cdot d \ [\mathrm{kN/m}]$$

$$\xi = 1 + \sqrt{\frac{200 \ [mm]}{d}}$$

(Eq. 12)

$$v_{\mathrm{Rd,min}} = \left(0{,}035 \cdot \xi^{3/2} \cdot f_c\right)^{1/2}$$

Where:

- $C_{\mathrm{Rd,c}}$ is a factor that depends on experimental tests (in Sweden $C_{\mathrm{Rd,c}} = 0{,}18$)
- d is the effective depth
- ξ is a factor accounting for the size effect
- ρ_l is the flexural reinforcement ratio, $\rho_l \leq 0{,}02$
- f_c is the compressive strength of concrete measured on cylinders.

BBK94 (Boverket, 1994)

The nominal shear strength ($v_{\mathrm{Rd,BBK}}$) is calculated according to **Eq. 13**. The critical cross section is considered to be at a distance of $d/2$. The influence of a tapered height is expressed as means of a term v_i depending on the bending moment M_d and a lever arm computed as d **(Eq. 14-15)**.

$$V_{\mathrm{Rd,BBK}} = \xi_{\mathrm{BBK}} \cdot (1 + 50 \cdot \rho_l) \cdot 0{,}30 \cdot f_{\mathrm{ct}} \cdot d \cdot b_0$$
$$v_{\mathrm{Rd,BBK}} = \xi_{\mathrm{BBK}} \cdot (1 + 50 \cdot \rho_l) \cdot 0{,}30 \cdot f_{\mathrm{ct}} \cdot d$$

$$\xi_{\mathrm{BBK}} = \begin{cases} 1{,}4 & \text{for } d \leq 0{,}2 \\ 1{,}6 - d & \text{for } 0{,}2 < d \leq 0{,}5 \\ 1{,}3 - 0{,}4d & \text{for } 0{,}5 < d \leq 1 \\ 0{,}9 & \text{for } d > 1 \end{cases}$$

(Eq. 13)

$$v_{\mathrm{Rd,eff}} = v_{\mathrm{Rd}} + v_i \ [\mathrm{kN/m}]$$

(Eq. 14)

$$v_i = \frac{M_d}{d} \tan \alpha = \frac{M}{d} \frac{(t_2 - t_1)}{a} \ [\mathrm{kN/m}]$$

(Eq. 15)

List of Bulletins from the Department of Structural Engineering, The Royal Institute of Technology, Stockholm

TRITA-BKN. Bulletin

Pacoste, C., On the Application of Catastrophe Theory to Stability Analyses of Elastic Structures.
Doctoral Thesis, 1993. Bulletin 1.

Stenmark, A-K., Dämpning av 13 m lång stålbalk – "Ullevibalken". Utprovning av dämpmassor och fastsättning av motbalk samt experimentell bestämning av modformer och förlustfaktorer. Vibration tests of full-scale steel girder to determine optimum passive control.
Licentiatavhandling, 1993. Bulletin 2.

Silfwerbrand, J., Renovering av asfaltgolv med cementbundna plastmodifierade avjämningsmassor.
1993. Bulletin 3.

Norlin, B., Two-Layered Composite Beams with Nonlinear Connectors and Geometry – Tests and Theory.
Doctoral Thesis, 1993. Bulletin 4.

Habtezion, T., On the Behaviour of Equilibrium Near Critical States.
Licentiate Thesis, 1993. Bulletin 5.

Krus, J., Hållfasthet hos frostnedbruten betong.
Licentiatavhandling, 1993. Bulletin 6.

Wiberg, U., Material Characterization and Defect Detection by Quantitative Ultrasonics.
Doctoral Thesis, 1993. Bulletin 7.

Lidström, T., Finite Element Modelling Supported by Object Oriented Methods.
Licentiate Thesis, 1993. Bulletin 8.

Hallgren, M., Flexural and Shear Capacity of Reinforced High Strength Concrete Beams without Stirrups. Licentiate Thesis, 1994. Bulletin 9.

Krus, J., Betongbalkars lastkapacitet efter miljöbelastning.
1994. Bulletin 10.

Sandahl, P., Analysis Sensitivity for Wind-related Fatigue in Lattice Structures.
Licentiate Thesis, 1994. Bulletin 11.

Sanne, L., Information Transfer Analysis and Modelling of the Structural Steel Construction Process.
Licentiate Thesis, 1994. Bulletin 12.

Zhitao, H., Influence of Web Buckling on Fatigue Life of Thin-Walled Columns.
Doctoral Thesis, 1994. Bulletin 13.

Kjörling, M., Dynamic response of railway track components. Measurements during train passage and dynamic laboratory loading.
Licentiate Thesis, 1995. Bulletin 14.

Yang, L., On Analysis Methods for Reinforced Concrete Structures.
Doctoral Thesis, 1995. Bulletin 15.

Petersson, Ö., Svensk metod för dimensionering av betongvägar.
Licentiatavhandling, 1996. Bulletin 16.

Lidström, T., Computational Methods for Finite Element Instability Analyses.
Doctoral Thesis, 1996. Bulletin 17.

Krus, J., Environment- and Function-induced Degradation of Concrete Structures.
Doctoral Thesis, 1996. Bulletin 18.

Editor, Silfwerbrand, J., Structural Loadings in the 21st Century.
Sven Sahlin Workshop, June 1996. Proceedings. Bulletin 19.

Ansell, A., Frequency Dependent Matrices for Dynamic Analysis of Frame Type Structures.
Licentiate Thesis, 1996. Bulletin 20.

Troive, S., Optimering av åtgärder för ökad livslängd hos infrastrukturkonstruktioner.
Licentiatavhandling, 1996. Bulletin 21.

Karoumi, R., Dynamic Response of Cable-Stayed Bridges Subjected to Moving Vehicles.
Licentiate Thesis, 1996. Bulletin 22.

Hallgren, M., Punching Shear Capacity of Reinforced High Strength Concrete Slabs.
Doctoral Thesis, 1996. Bulletin 23.

Hellgren, M., Strength of Bolt-Channel and Screw-Groove Joints in Aluminium Extrusions.
Licentiate Thesis, 1996. Bulletin 24.

Yagi, T., Wind-induced Instabilities of Structures.
Doctoral Thesis, 1997. Bulletin 25.

Eriksson, A., and Sandberg, G., (editors), Engineering Structures and Extreme Events – proceedings
from a symposium, May 1997. Bulletin 26.

Paulsson, J., Effects of Repairs on the Remaining Life of Concrete Bridge Decks.
Licentiate Thesis, 1997. Bulletin 27.

Olsson, A., Object-oriented finite element algorithms.
Licentiate Thesis, 1997. Bulletin 28.

Yunhua, L., On Shear Locking in Finite Elements.
Licentiate Thesis, 1997. Bulletin 29.

Ekman, M., Sprickor i betongkonstruktioner och dess inverkan på beständigheten.
Licentiate Thesis, 1997. Bulletin 30.

Karawajczyk, E., Finite Element Approach to the Mechanics of Track-Deck Systems.
Licentiate Thesis, 1997. Bulletin 31.

Fransson, H., Rotation Capacity of Reinforced High Strength Concrete Beams.
Licentiate Thesis, 1997. Bulletin 32.

Edlund, S., Arbitrary Thin-Walled Cross Sections. Theory and Computer Implementation.
Licentiate Thesis, 1997. Bulletin 33.

Forsell, K., Dynamic analyses of static instability phenomena.
Licentiate Thesis, 1997. Bulletin 34.

Ikäheimonen, J., Construction Loads on Shores and Stability of Horizontal Formworks.
Doctoral Thesis, 1997. Bulletin 35.

Racutanu, G., Konstbyggnaders reella livslängd.
Licentiatavhandling, 1997. Bulletin 36.

Appelqvist, I., Sammanbyggnad. Datastrukturer och utveckling av ett IT-stöd för byggprocessen.
Licentiatavhandling, 1997. Bulletin 37.

Alavizadeh-Farhang, A., Plain and Steel Fibre Reinforced Concrete Beams Subjected to Combined Mechanical and Thermal Loading.
Licentiate Thesis, 1998. Bulletin 38.

Eriksson, A. and Pacoste, C., (editors), Proceedings of the NSCM-11: Nordic Seminar on Computational Mechanics, October 1998. Bulletin 39.

Luo, Y., On some Finite Element Formulations in Structural Mechanics.
Doctoral Thesis, 1998. Bulletin 40.

Troive, S., Structural LCC Design of Concrete Bridges.
Doctoral Thesis, 1998. Bulletin 41.

Tärno, I., Effects of Contour Ellipticity upon Structural Behaviour of Hyparform Suspended Roofs.
Licentiate Thesis, 1998. Bulletin 42.

Hassanzadeh, G., Betongplattor på pelare. Förstärkningsmetoder och dimensioneringsmetoder för plattor med icke vidhäftande spännarmering.
Licentiatavhandling, 1998. Bulletin 43.

Karoumi, R., Response of Cable-Stayed and Suspension Bridges to Moving Vehicles. Analysis methods and practical modeling techniques.
Doctoral Thesis, 1998. Bulletin 44.

Johnson, R., Progression of the Dynamic Properties of Large Suspension Bridges during Construction − A Case Study of the Höga Kusten Bridge.
Licentiate Thesis, 1999. Bulletin 45.

Tibert, G., Numerical Analyses of Cable Roof Structures.
Licentiate Thesis, 1999. Bulletin 46.

Ahlenius, E., Explosionslaster och infrastrukturkonstruktioner - Risker, värderingar och kostnader.
Licentiatavhandling, 1999. Bulletin 47.

Battini, J-M., Plastic instability of plane frames using a co-rotational approach.
Licentiate Thesis, 1999. Bulletin 48.

Ay, L., Using Steel Fiber Reinforced High Performance Concrete in the Industrialization of Bridge Structures.
Licentiate Thesis, 1999. Bulletin 49.

Paulsson-Tralla, J., Service Life of Repaired Concrete Bridge Decks.
Doctoral Thesis, 1999. Bulletin 50.

Billberg, P., Some rheology aspects on fine mortar part of concrete.
Licentiate Thesis, 1999. Bulletin 51.

Ansell, A., Dynamically Loaded Rock Reinforcement.
Doctoral Thesis, 1999. Bulletin 52.

Forsell, K., Instability analyses of structures under dynamic loads.
Doctoral Thesis, 2000. Bulletin 53.

Edlund, S., Buckling of T-Section Beam-Columns in Aluminium with or without Transverse Welds.
Doctoral Thesis, 2000. Bulletin 54.

Löfsjögård, M., Functional Properties of Concrete Roads − General Interrelationships and Studies on Pavement Brightness and Sawcutting Times for Joints.
Licentiate Thesis, 2000. Bulletin 55.

Nilsson, U., Load bearing capacity of steel fibree reinforced shotcrete linings.
Licentiate Thesis, 2000. Bulletin 56.

Silfwerbrand, J. and Hassanzadeh, G., (editors), International Workshop on Punching Shear Capacity of RC Slabs − Proceedings. Dedicated to Professor Sven Kinnunen. Stockholm June 7-9, 2000. Bulletin 57.

Wiberg, A., Strengthening and repair of structural concrete with advanced, cementitious composites. Licentiate Thesis, 2000. Bulletin 58.

Racutanu, G., The Real Service Life of Swedish Road Bridges - A case study.
Doctoral Thesis, 2000. Bulletin 59.

Alavizadeh-Farhang, A., Concrete Structures Subjected to Combined Mechanical and Thermal Loading.
Doctoral Thesis, 2000. Bulletin 60.

Wäppling, M., Behaviour of Concrete Block Pavements - Field Tests and Surveys.
Licentiate Thesis, 2000. Bulletin 61.

Getachew, A., Trafiklaster på broar. Analys av insamlade och Monte Carlo genererade fordonsdata.
Licentiatavhandling, 2000. Bulletin 62.

James, G., Raising Allowable Axle Loads on Railway Bridges using Simulation and Field Data.
Licentiate Thesis, 2001. Bulletin 63.

Karawajczyk, E., Finite Elements Simulations of Integral Bridge Behaviour.
Doctoral Thesis, 2001. Bulletin 64.

Thöyrä, T., Strength of Slotted Steel Studs.
Licentiate Thesis, 2001. Bulletin 65.

Tranvik, P., Dynamic Behaviour under Wind Loading of a 90 m Steel Chimney.
Licentiate Thesis, 2001. Bulletin 66.

Ullman, R., Buckling of Aluminium Girders with Corrugated Webs.
Licentiate Thesis, 2002. Bulletin 67.

Getachew, A., Traffic Load Effects on Bridges. Statistical Analysis of Collected and Monte Carlo Simulated Vehicle Data.
Doctoral Thesis, 2003. Bulletin 68.

Quilligan, M., Bridge Weigh-in-Motion. Development of a 2-D Multi-Vehicle Algorithm.
Licentiate Thesis, 2003. Bulletin 69.

James, G., Analysis of Traffic Load Effects on Railway Bridges.
Doctoral Thesis 2003. Bulletin 70.

Nilsson, U., Structural behaviour of fibre reinforced sprayed concrete anchored in rock.
Doctoral Thesis 2003. Bulletin 71.

Wiberg, A., Strengthening of Concrete Beams Using Cementitious Carbon Fibre Composites.
Doctoral Thesis 2003. Bulletin 72.

Löfsjögård, M., Functional Properties of Concrete Roads – Development of an Optimisation Model and Studies on Road Lighting Design and Joint Performance.
Doctoral Thesis 2003. Bulletin 73.

Bayoglu-Flener, E., Soil-Structure Interaction for Integral Bridges and Culverts.
Licentiate Thesis 2004. Bulletin 74.

Lutfi, A., Steel Fibrous Cement Based Composites. Part one: Material and mechanical properties.
Part two: Behaviour in the anchorage zones of prestressed bridges.
Doctoral Thesis 2004. Bulletin 75.

Johansson, U., Fatigue Tests and Analysis of Reinforced Concrete Bridge Deck Models.
Licentiate Thesis 2004. Bulletin 76.

Roth, T., Langzeitverhalten von Spannstählen in Betonkonstruktionen.
Licentitate Thesis 2004. Bulletin 77.

Hedebratt, J., Integrerad projektering och produktion av industrigolv – Metoder för att förbättra kvaliteten.
Licentiatavhandling, 2004. Bulletin 78.

Österberg, E., Revealing of age-related deterioration of prestressed reinforced concrete containments in nuclear power plants – Requirements and NDT methods.
Licentiate Thesis 2004. Bulletin 79.

Broms, C.E., Concrete flat slabs and footings New design method for punching and detailing for ductility.
Doctoral Thesis 2005. Bulletin 80.

Wiberg, J., Bridge Monitoring to Allow for Reliable Dynamic FE Modelling - A Case Study of the New Årsta Railway Bridge.
Licentiate Thesis 2006. Bulletin 81.

Mattsson, H-Å., Funktionsentreprenad Brounderhåll – En pilotstudie i Uppsala län.
Licentiate Thesis 2006. Bulletin 82.

Masanja, D. P, Foam concrete as a structural material.
Doctoral Thesis 2006. Bulletin 83.

Johansson, A., Impregnation of Concrete Structures – Transportation and Fixation of Moisture in Water Repellent Treated Concrete.
Licentiate Thesis 2006. Bulletin 84.

Billberg, P., Form Pressure Generated by Self-Compacting Concrete – Influence of Thixotropy and Structural Behaviour at Rest.
Doctoral Thesis 2006. Bulletin 85.

Enckell, M., Structural Health Monitoring using Modern Sensor Technology – Long-term Monitoring of the New Årsta Railway Bridge.
Licentiate Thesis 2006. Bulletin 86.

Söderqvist, J., Design of Concrete Pavements – Design Criteria for Plain and Lean Concrete.
Licentiate Thesis 2006. Bulletin 87.

Malm, R., Shear cracks in concrete structures subjected to in-plane stresses.
Licentiate Thesis 2006. Bulletin 88.

Skoglund, P., Chloride Transport and Reinforcement Corrosion in the Vicinity of the Transition Zone between Substrate and Repair Concrete.
Licentiate Thesis 2006. Bulletin 89.

Liljencrantz, A., Monitoring railway traffic loads using Bridge Weight-in-Motion.
Licentiate Thesis 2007. Bulletin 90.

Stenbeck, T., Promoting Innovation in Transportation Infrastructure Maintenance – Incentives, Contracting and Performance-Based Specifications.
Doctoral Thesis 2007. Bulletin 91

Magnusson, J., Structural Concrete Elements Subjected to Air Blast Loading.
Licentiate Thesis 2007. Bulletin 92.

Pettersson, L., G., Full Scale Tests and Structural Evaluation of Soil Steel Flexible Culverts with low Height of Cover.
Doctoral Thesis 2007. Bulletin 93

Westerberg, B., Time-dependent effects in the analysis and design of slender concrete compression members.
Doctoral Thesis 2008. Bulletin 94

Mattsson, H-Å, Integrated Bridge Maintenance. Evaluation of a pilot project and future perspectives.
Doctoral Thesis 2008. Bulletin 95

Andersson, A., Utmattningsanalys av järnvägsbroar. En fallstudie av stålbroarna mellan Stockholm Central och Söder Mälarstrand, baserat på teoretiska analyser och töjningsmätningar.
Licentiate Thesis 2009. Bulletin 96

Malm, R., Predicting shear type crack initiation and growth in concrete with non-linear finite element method.
Doctoral Thesis 2009. Bulletin 97

Bayoglu Flener, E., Static and dynamic behavior of soil-steel composite bridges obtained by field testing.
Doctoral Thesis 2009. Bulletin 98

Gram, A., Numerical Modelling of Self-Compacting Concrete Flow
Licentiate Thesis 2009. Bulletin 99

Wiberg, J., Railway bridge response to passing trains. Measurements and FE model updating.
Doctoral Thesis 2009. Bulletin 100

Athuman M.K. Ngoma, Characterisation and Consolidation of Historical Lime Mortars in Cultural Heritage Buildings and Associated Structures in East Africa.
Doctoral Thesis 2009. Bulletin 101

Ülker-Kaustell, M., Some aspects of the dynamic soil-structure interaction of a portal frame railway bridge.
Licentiate Thesis 2009. Bulletin 102

Vogt, C., Ultrafine particles in concrete
Doctoral Thesis 2010. Bulletin 103

Selander, A., Hydrophobic Impregnation of Concrete Structures
Doctoral Thesis 2010. Bulletin 104

Ilina, E., Understanding the application of knowledge management to safety critical facilities
Doctoral Thesis 2010. Bulletin 105

Leander, J., Improving a bridge fatigue life prediction by monitoring
Licentiate Thesis 2010. Bulletin 106

Andersson, A., Capacity assessment of arch bridges with backfill – Case of the old Årsta railway bridge
Doctoral Thesis 2011. Bulletin 107

Enckell, M., Lessons Learned in Structural Health Monitoring of Bridges Using Advanced Sensor Technology
Doctoral Thesis 2011. Bulletin 108

Hansson, H., Warhead penetration in concrete protective structures
Licentiate Thesis 2011. Bulletin 109

Gonzalez Silva, I., Study and Application of Modern Bridge Monitoring Techniques
Licentiate Thesis 2011. Bulletin 110

Safi, M., LCC Applications for Bridges and Integration with BMS
Licentiate Thesis 2012. Bulletin 111

Guangli, D., Towards sustainable construction, life cycle assessment of railway bridges
Licentiate Thesis 2012. Bulletin 112

Hedebratt, J., Industrial Fibre Concrete Slabs – Experiences and Tests on Pile-Supported Slab
Doctoral Thesis 2012. Bulletin 113

Ahmed, L., Models for analysis of shotcrete on rock exposed to blasting
Licentiate Thesis 2012. Bulletin 114

Le, T., N., Corotational formulation for nonlinear dynamic analysis of flexible beam structures
Licentiate Thesis 2012. Bulletin 115

Johansson, C., Simplified dynamic analysis of railway bridges under high-speed trains
Licentiate Thesis 2013. Bulletin 116

Jansson, R., Fire Spalling of Concrete – Theoretical and Experimental Studies
Doctoral Thesis 2013. Bulletin 117

Leander, J., Refining the fatigue assessment procedure of existing steel bridges
Doctoral Thesis 2013. Bulletin 118

Le, T., N., Nonlinear dynamics of flexible structures using corotational beam elements
Doctoral Thesis 2013. Bulletin 119

Ülker-Kaustell, M., Essential modelling details in dynamic FE-analyses of railway bridges
Doctoral Thesis 2013. Bulletin 120

Safi, M., Life-Cycle Costing. Applications and Implementations in Bridge Investment and Management
Doctoral Thesis 2013. Bulletin 121

Arvidsson, T., Train-Bridge Interaction: Literature Review and Parameter Screening
Licentiate Thesis 2014. Bulletin 122

Rydell, C., Seismic high-frequency content loads on structures and components within nuclear facilities
Licentiate Thesis 2014. Bulletin 123

Bryne, L. E., Time dependent material properties of shotcrete for hard rock tunnelling
Doctoral Thesis 2014. Bulletin 124

Wennström, J., Life Cycle Costing in Road Planning and Management: A Case Study on Collisionfree Roads
Licentiate Thesis 2014. Bulletin 125

Gonzalez Silva, I., Application of monitoring to dynamic characterization and damage detection in bridges
Doctoral Thesis 2014. Bulletin 126

Sangiorgio, F., Safety Format for Non-linear Analysis of RC Structures Subjected to Multiple Failure Modes
Doctoral Thesis 2015. Bulletin 127

Gram, A., Modelling of Cementitious Suspensial Flow – Influence of Viscosity and Aggregate Properties
Doctoral Thesis 2015. Bulletin 128

Du, G., Life Cycle Assessment of bridges, model development and Case Studies
Doctoral Thesis 2015. Bulletin 129

Zhu, J., Towards a Viscoelastic Model for Phase Separation in Polymer Modified Bitumen
Licentiate Thesis 2015. Bulletin 130

Chen, F., The Future of Smart Road Infrastructure. A Case Study for the eRoad.
Licentiate Thesis 2015. Bulletin 131

Ahmed, L., Models for analysis of young cast and sprayed concrete subjected to impact-type loads
Doctoral Thesis 2015. Bulletin 132

Albrektsson, J., Durability of Fire Exposed Concrete – Experimental Studies Focusing on Stiffness &
Transport Properties
Licentiate Thesis 2015. Bulletin 133

Wallin, J., Systematic planning and execution of finite element model updating
Licentiate Thesis 2015. Bulletin 134

Wadi, A.,Flexible Culverts in Sloping Terrain
Licentiate Thesis 2015. Bulletin 135

McCarthy, R., Self-Compacting Concrete for Improved Construction Technology
Licentiate Thesis 2015. Bulletin 136

The department also publishes other series. For full information see our homepage http://www.byv.kth.se

www.kth.se